INVESTIGATION ON ULTRASONIC P-WAVE VELOCITY AND ATTENUATION PARAMETERS FOR SULFATE DEGRADED CONCRETE

By

MEHER SRI LALITHA MANDAVILLI

Bachelor of Science in Civil Engineering

Osmania University

Hyderabad, Telangana - India.

2012

Submitted to the Faculty of the
Graduate College of the
Oklahoma State University
in partial fulfillment of
the requirements for
the Degree of
MASTER OF SCIENCE
July, 2015

INVESTIGATION ON ULTRASONIC P-WAVE VELOCITY AND ATTENUATION PARAMETERS FOR SULFATE DEGRADED CONCRETE

Thesis Approved:

Dr. Julie Ann Hartell

Thesis Adviser

Dr. M. Tyler Ley

Committee Member

Dr. Robert N. Emerson

Committee Member

ACKNOWLEDGEMENTS

First and foremost I would like to express my deepest gratitude to my advisor, Dr. Julie Ann Hartell. I appreciate all her contributions of time, ideas, and funding to make my Master's experience productive and stimulating. The joy and enthusiasm she has for her research was contagious and motivational for me, even during tough times in the Master's pursuit. I am also thankful for the excellent example she has provided as a successful woman.

I would like to thank my committee member Dr. Tyler Ley for his consistent support and guidance throughout my Master's degree.

In full gratitude I would like to acknowledge my friends, Ignatius Vasant, Harishma Donthineni and Wassay Gulrez who encouraged, inspired, supported and assisted me in my pursuit of Master's degree. I would like to thank my friends for making the group cheerful and bringing a lot of fun, both inside and outside the lab. Without their guidance and persistent help this dissertation would not have been possible.

Most importantly, none of this would have been possible without the love and patience of my family. I would like to thank and dedicate this dissertation to my parents, Mr. Meher Mallikarjun and Mrs. Valli Subhadra for their love and support throughout my life. Thank you both for giving me strength to reach for the stars and chase my dreams. My siblings, Mrs. Meher Lakshmi and Mr. Shiva Meher and brother-in-law, Mr. Nikunj Vihari deserve my wholehearted thanks as well. You all made me who I am now.

Name: MEHER SRI LALITHA MANDAVILLI

Date of Degree: JULY, 2015

Title of Study: INVESTIGATION ON ULTRASONIC P-WAVE VELOCITY AND ATTENUATION PARAMETERS FOR SULFATE DEGRADED CONCRETE

Major Field: CIVIL ENGINEERING

Abstract:

Concrete durability is affected due to various deterioration mechanisms. Sulfate attack on concrete is one of the major reasons for loss in mechanical properties of concrete and causes spalling and cracking. It is a mechanism, which causes a chemical break down within the concrete wherein the sulfate ions combines with C-S-H forming ettringite which destroys the cement paste (Mishra 2014).

Ultrasonic pulse emission techniques was used to evaluate the extent of degradation due to external sulfate attack. In this study, the wave velocity and wave attenuation measurements are considered for the degradation analysis. The specimens were subjected to “diffusion” exposure regimen in two different solutions namely limewater (LW) and 5% sodium sulfate solution. The diametric velocities and attenuation were then calculated for a 300 kHz transient wave. This study shows that velocity decreases over time and exposure due to the degradation of concrete paste by the sulfate. But, no change in attenuation is observed in this study. This may be due to aggregates not being affected by the sulfate exposure (as attenuation depends on aggregate degradation).

TABLE OF CONTENTS

LIST OF TABLES

LIST OF FIGURES

CHAPTER 1

INTRODUCTION

In the modern years, deterioration of concrete structures such as bridges and buildings has been a problem. Proper inspection techniques for deteriorated structures are vital in making decisions regarding rehabilitation, repair or replacement. Therefore, the advancements in techniques to evaluate degradation of structures under various exposure conditions has been one of the major issues for a good maintenance program (Yuyama et al., 1999).

Ultrasonic pulse emission technique is broadly applied to various fields in civil engineering including investigation of concrete materials. Concrete is a heterogeneous material made of cement, fine aggregate, coarse aggregates and air bubbles which makes the material characterization a complicated task. The understanding of the ultrasound interaction with the various phases in the suspension is a first step in order to correctly interpret stress wave propagation data (Aggelis and Philippidis 2004). As such, many studies have been conducted on the use of ultrasonic pulse emission techniques to evaluate the integrity of concrete structures which are partly summarized in Chapter 2, Literature Review.

In this study, ultrasonic testing was performed to evaluate the extent of concrete degradation due to external sulfate attack. Herein, wave velocity and wave attenuation measurements are analyzed to determine whether these can be used as viable parameters to determine the extent of

sulfate degradation. To accomplish such, a research methodology (Chapter 3) was devised which comprised of making numerous concrete samples to be immersed in a 5% sodium sulfate solution for periods of 3, 6, 12, 18 and 24 months. Then, extensive ultrasonic nondestructive testing was performed on these specimens to evaluate the extent of damage in time.

The results obtained are presented and discussed in Chapter 4. These demonstrates how sensitive the test method is in measuring changes in concrete mechanical behaviors due to sulfate exposure. The significant contributions and major observations of this study are summarized in Chapter 5.

CHAPTER 2

REVIEW OF LITERATURE

Ultrasonic pulse velocity is a non-destructive technique (NDT) based on stress wave propagation and it is used to evaluate concrete performance. By analyzing the changes in ultrasonic signals traveling through a concrete material, parameters such as porosity, strength and deterioration of concrete can be evaluated (Malhotra and Cario 1991; Uomoto 2000). However, concrete is a inhomogeneous material consisting of cement, fine and coarse aggregate, air bubbles and water; and ultrasonic results are differently affected by each individual component. The mechanism of how ultrasonic waves interact with the various phases of the material has to be thoroughly studied to establish a relationship between wave propagation parameters and concrete material properties. The dispersive and attenuative nature of inhomogeneous concrete may enhance the capabilities of the NDT method to interpret results obtained (Philippidis and Aggelis 2004). This chapter provides insight on past research carried out on stress wave propagation theory and ultrasonic methodology.

2.1 Stress – Wave Methods for Structures

Stress-wave propagation theory is currently being used in several nondestructive testing methods. NDT techniques such as through-wave velocity, pulse-echo, impact-echo, and impulse response and spectrum analysis of surface waves (SASW) are popular techniques which help to understand the internal conditions of the structure. The ultrasonic pulse velocity method can be used for flaw

detection and thickness measurement by measuring the time taken for a wave to travel through a member. This is based on the stress-wave propagation principle, *"A disturbance on a solid causes the entire body to respond by linear and angular accelerations"* (Sadri and Mirkhani 2009).

Deformation in a body is caused by applied forces. Similarly, stress-waves are generated only when a force is applied rapidly and the resulting deformation is an elastic response. Three types of stress waves are observed: P waves, S waves and R waves (shown in Figure 1). P waves, also called compression waves, results in a particle motion parallel to the direction of propagation of the wave and are the results of compressive or tensile stresses. In S waves, also called as Shear waves, the particle motion and direction of propagation are perpendicular to each other and these produce shear stress. In R waves, also called Rayleigh waves, the propagation of stress waves is through the surface of the solid.

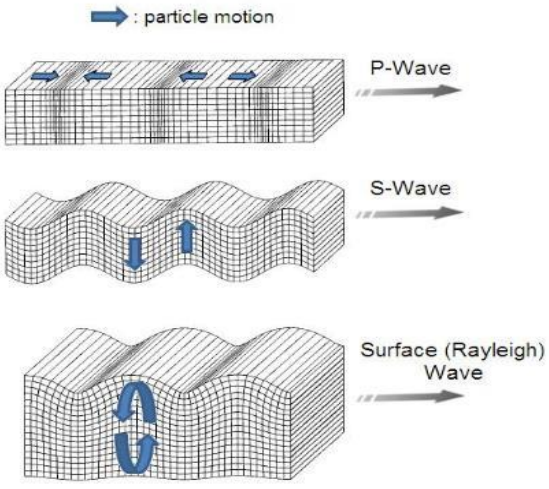

Figure 1: Various types of stress wave propagations

(Source: http://www.parkseismic.com/Whatisseismicwave.html)

The velocity at which a wave travels through a medium is governed by the following fundamental equation Eq. 1: (Sadri and Mirkhani 2009)

$$C = f \times \lambda \quad \text{...Eq. 1}$$

Where,

C: wave velocity

f: wave frequency

λ: wavelength

The velocity of a stress wave depends on the density and the elastic properties of the material. The P wave velocity is calculated using the following equation Eq. 2: (Sadri and Mirkhani 2009)

$$C_p = \sqrt{\frac{E(1-v)}{(1+v)(1-2v)\rho}} \quad \text{...Eq. 2}$$

Where,

E: Young's modulus

C_p: P wave velocity

ρ: density

v: Poisson's ratio

S-wave velocity is as follows Eq. 3: (Sadri and Mirkhani 2009)

$$C_s = \sqrt{\frac{E}{2(1+v)\rho}} \quad \text{...Eq. 3}$$

R-wave velocity can be determined by Eq. 4: (Sadri and Mirkhani 2009)

$$C_r = \frac{0.87+1.12v}{1+v} C_s \quad \text{...Eq. 4}$$

Refraction, reflection and mode conversion of the waves are caused when the stress waves encounter an acoustic interface, which is defined as the boundary between materials with different acoustic impedances. Acoustic impedance is given by Eq.5: (Sadri and Mirkhani 2009)

$$Z = \rho \times C_p \quad \text{...Eq. 5}$$

For compression waves with a normal angle of incidence, the reflected and the incident waves are given by the following Eq. 6: (Sadri and Mirkhani 2009)

$$R_p = I_p \times \frac{Z_2 - Z_1}{Z_2 - Z_1} \quad \text{...Eq. 6}$$

Where,

I_p = Stress related to incident P waves

R_p = Stress related to reflected P waves

Z_1 = Acoustic Impedance of Medium 1

Z_2 = Acoustic Impedance of Medium 2

2.2 Ultrasonic Through Transmission Method

This is one of the oldest NDT techniques and measures based on the travel time for the ultrasonic waves to travel over a known path length. This is also called the Ultrasonic Pulse Velocity (UPV) method. The speed of wave propagation depends on the elastic properties and density of concrete. The variations in density may be due to improper consolidations and that for elastic properties may be due to material variations, mix proportions and curing. The determination of stress wave

velocity at various locations in a structures gives information about the uniformity of the material. Thus, the wave speeds are determined by measuring the travel time over the known path length Eq. 7. The mechanism is shown in Figure 2(a) (Sadri and Mirkhani 2009).

$$C_p = \frac{X}{t} \quad \text{...Eq. 7}$$

Where,

x = distance between transducers

t = pulse travel time between transducers

This techniques is based on the relationship between concrete quality and velocity of the pulse through the material. The testing equipment consists of a transmitter, receiver and a digital waveform analyzer (shown in Figure 2(b)). Ultrasonic pulse travels through the concrete of known thickness or between known distances between transducers (Sadri and Mirkhani 2009).

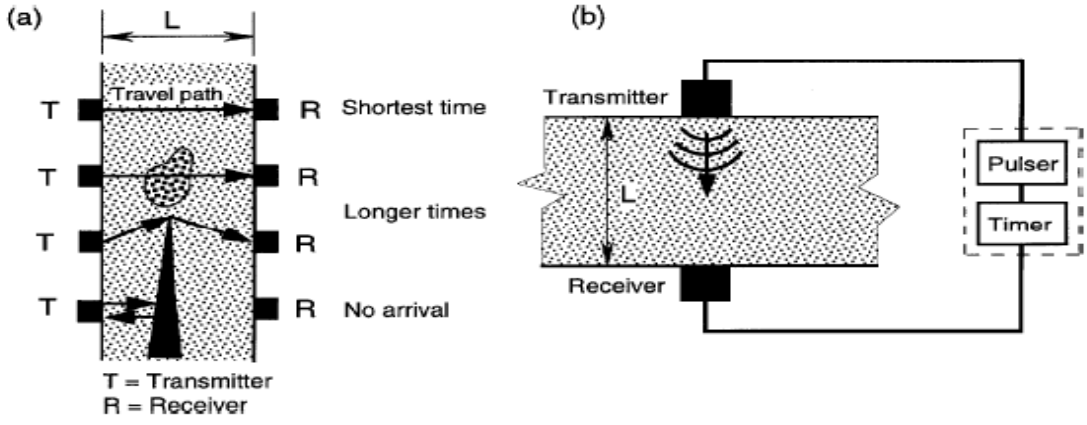

Figure 2: Ultrasonic pulse velocity mechanism

(ACI 228.2R-13)

Research has been done to correlate pulse velocity to compressive strength. As the pulse velocity is a function of material stiffness and density, these have been correlated with compressive strength (Sadri and Mirkhani 2009).

Based on stress – wave propagation theory non - destructive test methods could be used to measure the dynamic modulus of elasticity (Panzera et al. 2011). It was observed that there was a good agreement between average values of dynamic and static modulus. The variability observed in the dynamic values was less than the static values (Castro & Carino 1998; Vipulanandan & Garas 2008). The ultrasonic pulse frequency used for evaluating cementitious materials is from about 20 kHz to 250 kHz with wavelengths from 200 mm for lower frequencies to 16 mm at higher frequencies. The frequency of 50 kHz being suitable for field evaluation of concrete (Pundit 1990).

For homogeneous, elastic and isotropic material, the constrained modulus (defined as axial stress by axial strain in a uniaxial strain state) is given by Eq. 8 (Leslie & Chessman 1949):

$$M = \left[\frac{(1-\nu)}{(1+\nu)(1-2\nu)}\right] E \qquad \ldots\text{Eq.8}$$

Where,

M = Constrained modulus

ν = Poisson's ratio

E = Young's modulus

And, the dynamic young's modulus is given by Eq. 9 (Leslie & Chessman 1949) and relation is shown in figure 3,

$$E_p = \left[\frac{(1+\nu p)(1-2\nu p)}{(1-\nu p)}\right](\gamma/g)v_p^2 \quad \text{…Eq. 9}$$

Where,

E_p = Dynamic Young's modulus

v_p = Dynamic Poisson´s ratio

(γ/g) = Mass density of the material

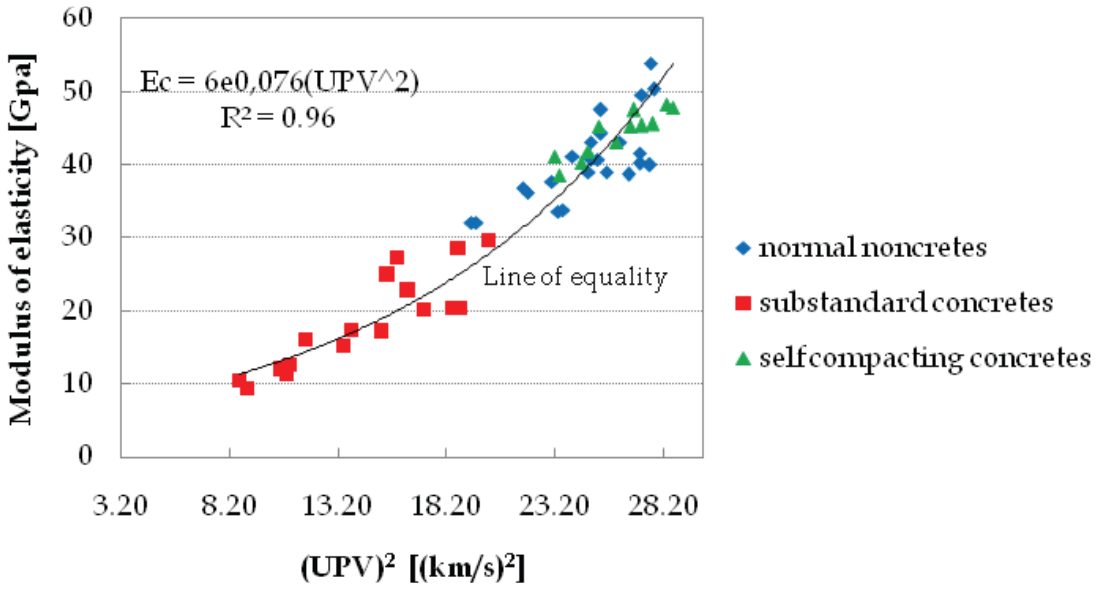

Figure 3: Relationship between UPV and E_s

(Yildirim and Sengul 2011)

The Ultrasonic pulse velocity depends on the elastic properties of the concrete such as stiffness, modulus of elasticity which is in turn responsible for the mechanical strength of the material. The correlation also depends on mix proportions, type of aggregate and cement type (Neville, 1996; Trtnik et al. 2009). Thus, ultrasonic pulse velocity could be used to estimate the compressive strength of concrete as long as the calibration curves for the assessed material is available (Mandandoust et al., 2010).

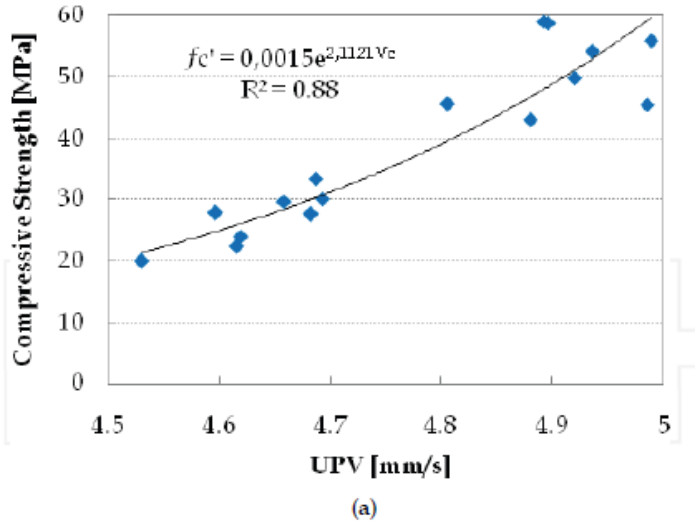

Figure 4: Correlation between Compressive strength and UPV for

(a) SCC with FA. (b) SCC with SF

(Ulucan et al. 2008)

Many correlations were established between compressive strength and pulse velocity of concrete. It was observed that there the relation between compressive strength and UPV measurements was

exponential for self-compacting cements (SCC) with both silica fume (SA) and fly ash (FA) (Figure 4). And, it was also noticed that the constants for each pozzalonic material differed with the amount of Portland cement replaced with self-compacting cement. Thus, UPV is an important non – destructive method and provides reliable results with quick measurements and also with cost effective equipment (Panzera et al. 2011).

Lawson et al., 2011 studied the relationship between ultrasonic pulse velocity and compressive strength of concrete. The concrete specimens used in this study were made with 18% paste content with different water to cement ratios and constituents. Destructive and non - destructive tests i.e., compressive strength test and ultrasonic pulse velocity tests were carried out on the specimens at 2, 7, 15 and 28 days. A curve representing the relation between ultrasonic pulse velocity and compressive tests was derived for water to cement ratios ranging between 0.35 and 0.70. Different correlation curves (Figure 5 – Figure 11) for ultrasonic pulse velocity and compressive strength of hardened concrete was established for concrete with water to cement ratio of 0.35, 0.4, 0.5, 0.6 and 0.7. It can be observed that as the age of the specimen increased, the UPV measurements and compressive strength also increased. At a particular age, a higher UPV and compressive strength was observed for specimens with lower water to cement ratio (Lawson et al. 2011).

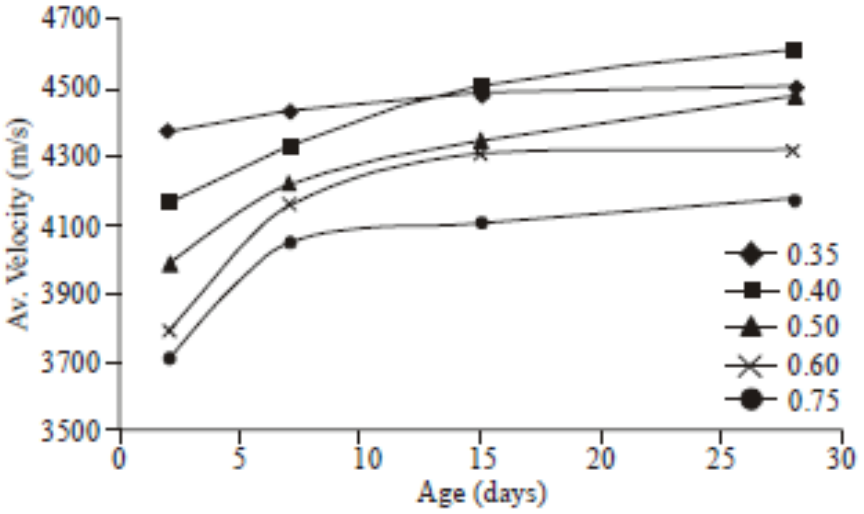

Figure 5: UPV of concrete cubes against age
(Lawson et al. 2011)

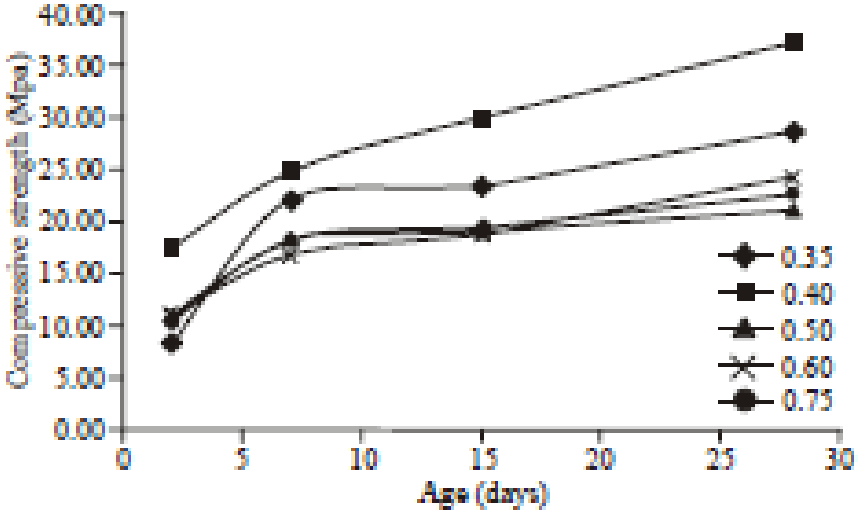

Figure 6: Compressive strength of concrete cubes against age.

(Lawson et al. 2011)

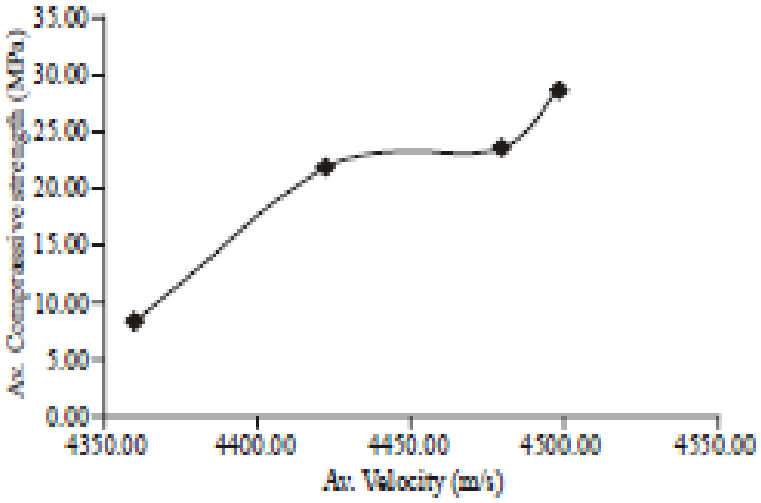

Figure 7: Comparison of average velocity and compressive strength of concrete cubes with 0.35 W/C.

(Lawson et al. 2011)

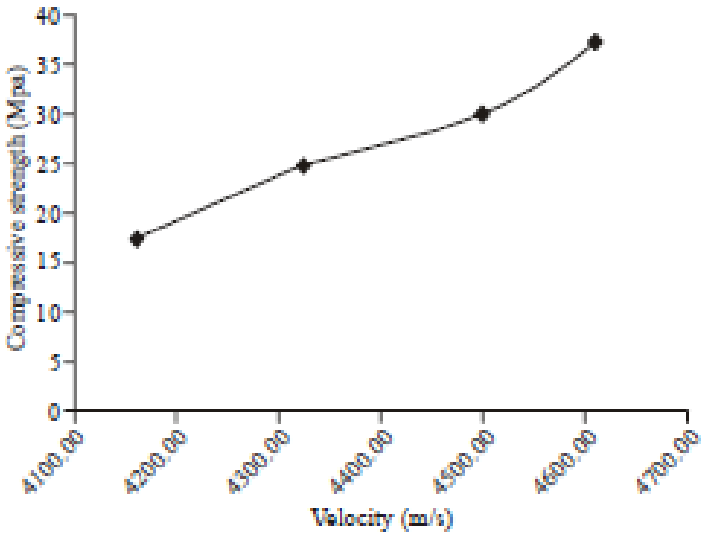

Figure 8: Comparison of average velocity and compressive strength of concrete cubes with 0.4 W/C.

(Lawson et al. 2011)

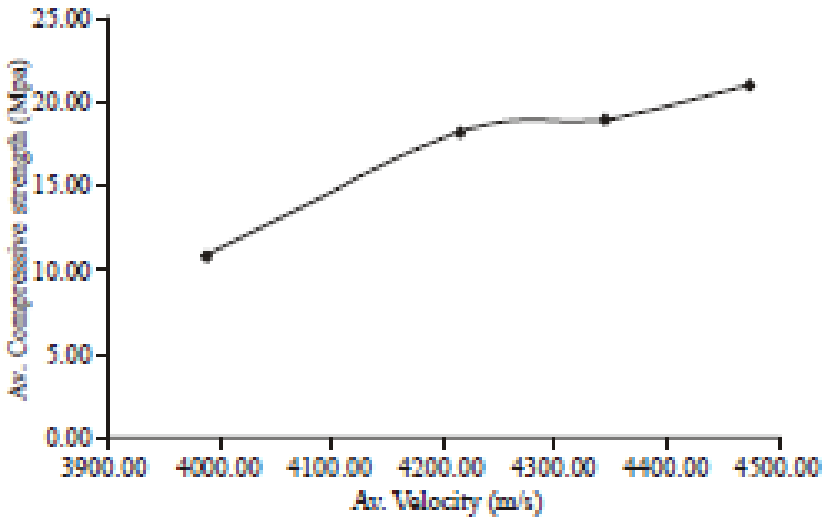

Figure 9: Comparison of average velocity and compressive strength of concrete cubes with 0.5 W/C.

(Lawson et al. 2011)

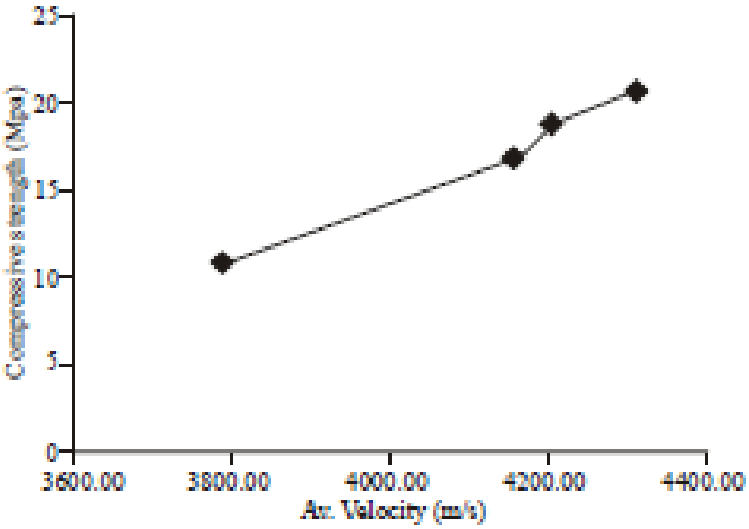

Figure 10: Comparison of average velocity and compressive strength of concrete cubes with 0.6 W/C.

(Lawson et al. 2011)

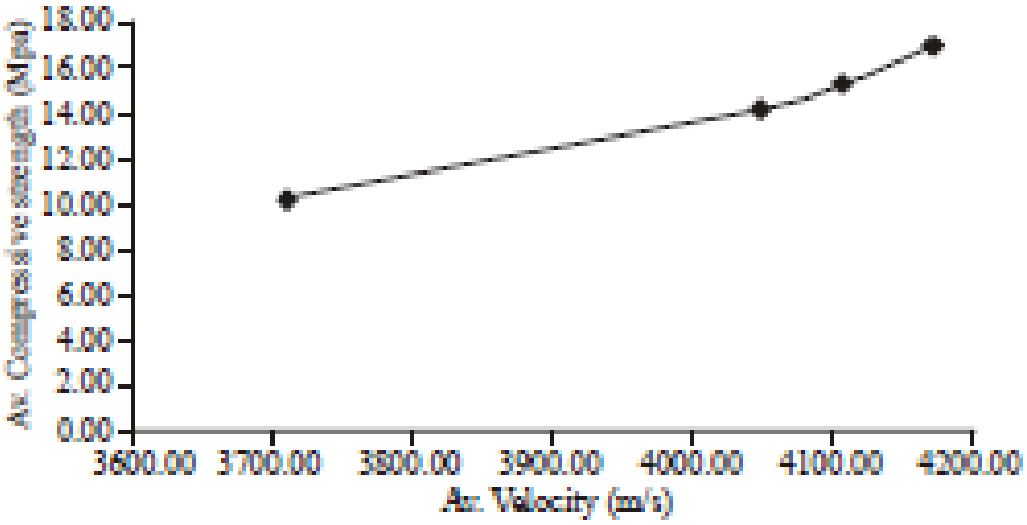

Figure 11: Comparison of average velocity and compressive strength of concrete cubes with 0.7 W/C.

(Lawson et al. 2011)

Equations are derived from the above shown curves and validation of these equation was carried out with different concrete mixture by evaluating their compressive strength through the equations (UPV measurements) and compressive testing. The results obtained by the UPV measurements deviated within ±10% from the compressive test (Lawson et al. 2011).

To improve this testing method, studies have been carried on the effects of wave attenuation on UPV measurements. These are focused on varying the concrete mixture, where many boundaries are generated increasing the material's inhomogeneity.

2.2.1 Ultrasonic Wave Attenuation

Philippidis and Aggelis (2004) showed that aggregates play a significant role in wave propagation considerably increasing the wave velocity, while the aggregate size controls the wave attenuation and the velocity variations with frequency in relation to inhomogeneity of the materials was discussed. The interaction of ultrasound waves with different phases should be thoroughly studied in order to establish a relation between propagation characteristics and material properties. A number of works shows that the attenuation does not seem to increase with the aggregate size and this particular behaviors is attributed to air bubbles present in cement paste or the presence of aggregates that act as "Larger homogeneous structures embedded in the matrix that facilitate the propagation of high frequencies" (Gaydecki et al. 1992). Philippidis and Aggelis (2004) examined that scattering loses are negligible compared to absorption loses. And it has been shown in many other works that an increase in aggregate content results in higher wave velocity.

To study the attenuative behavior of concrete, Philippidis and Aggelis (2004) prepared various mortar and concrete mixtures of different compositions and the attenuation coefficient was determined by measuring the reduction in amplitude of ultrasonic wave that has traveled a known distance through a material (Eq. 10).

$$\alpha = -\frac{20}{x}\log\left(\frac{A_x}{A_0}\right) \quad \text{...Eq. 10}$$

Where,

A_0 = initial amplitude

A_x = amplitude travelled after x distance

x = distance travelled (distance between sensors)

α = attenuation coefficient

Cement paste, mortar and concrete showed approximately constant value of attenuation for frequency above 200 kHz. It was found that the wave path needs to be larger than the wavelength of the pulse to get correct velocity values for the material studied. Therefore, it was concluded that the geometry of the specimen influences velocity measurements, but it was not the reason for the observed dispersion, which was attributed to the material. The aggregate content was a decisive parameter in the propagation behavior within mortar and concrete. The aggregate size has more impact on the attenuation behavior than on pulse velocity. The observed dispersion at low frequencies may be due to the inhomogeneous nature of concrete (Philippidis and Aggelis 2004).

A similar study was conducted for fresh mixtures. The wave propagation in fresh mortar was studied by Aggelis and Philippidis (2004) followed by an investigation on the quality estimation through composition control. The dispersive and attenuative nature of fresh cementitious material were observed from the results obtained from the tone-burst and sine-sweep experiments indicated. The role of the sand (inclusion) content in wave propagation affects both velocity and attenuation. Notable differences, in attenuation, were observed where sand rich mixes exhibit much higher attenuation than cement paste for frequencies above 300 kHz. The opposite was found for frequencies lower than 200 kHz. For lower frequencies, 80-90 kHz, a decrease in attenuation was observed and for higher frequencies, above 300 kHz, attenuation increases proportional to the sand content was also observed. Strong attenuation at low frequencies was also observed in specimens containing no aggregates, this is because of the presence of air bubbles, present in fresh mortar. It was also observed that the larger grain size resulted in higher

attenuation than fine sand, this lead to the assumption that scattering is the dominant form of attenuation mechanism.

Although ultrasonic testing has been effective in assessing deteriorated concrete, its attenuative behavior still poses a challenge in order to better understand ongoing degradation mechanisms. External sulfate attack, is an example where the observed change in mechanical properties, i.e. modulus of elasticity, over time may be sensitive to ultrasonic testing.

2.3 Overview of External Sulfate Attack

This section briefs earlier published work on sulfate attack on concrete. It details about the sources of sulfates, its effects on concrete durability, reactions that take place in the concrete and also the testing methods to recognize, classify and analyze the attack.

2.3.1 External Sulfates Attack Mechanism

The visual investigations of concrete exposed to sulfate compounds shows signs of degradation as in macro cracking, spalling and delamination. These degradations are due to the microstructural changes in concrete which are

- Loss of cementing properties
- Loss of Paste cohesion
- Loss of cement paste-aggregate bond

The microstructural changes are the result of physical processes and chemical reactions between hydrated cement paste and external sulfates compounds. A sodium sulfates attack may engage one, some or many of the following reactions:

- Dissolution, decomposition or exclusion of hydrated products and unhydrated elements.
- Ettringite (Figure 12), thaumasite and gypsum formation
- Repetitive recrystallization of sulfate salts
- Composite and constant changes in the composition (ionic) of the pore liquid phase.

(Skalny et al. 2002) (Neville 2004)

Figure 12: Ettringite (white, needle-like crystals) are commonly found in samples taken from concrete in service

(Stutzman 2001).

Sulfates decrease the durability of concrete and can shorten the life of a structure. The main sources of sulfates are:

- Sewage water or industrial waste - rich in sulfuric acid
- Sulfates compounds found in water sources such as lakes, rivers, seawater and groundwater.
- sulfide minerals oxidation in clay which is adjacent to the concrete (produce reactive sulfuric acid) (Winter 2005)

The deterioration of concrete is not exclusively because of the availability and concentration of sulfates, but is also inclined towards the transport mechanisms by which they may enter the porous medium (Skalny et al. 2002).

2.3.2 Transport Mechanisms

There are different processes that may cause deterioration of a concrete structure including, reinforcement corrosion, frost damage and sulfate attack. The deteriorations mechanism require transportation of water, oxygen, chemicals in and out of the concrete. In order to improve the durability of the structure a clear knowledge and understanding of the transport mechanisms is required. Four main transport mechanism are described: (Claisse 2014)

- Pressure driven flow
- Diffusion
- Electro migration
- Thermal migration.

In addition to the above external mechanisms, such as an applied pressure, there are also three important processes which are internal to the concrete: (Claisse 2014)

- Adsorption
- Capillary
- Osmosis

2.3.3 Testing Methods and Evaluation of Sulfate Attack

2.3.3.1 ASTM C 1012 Standard Evaluation

The standard method used in the industry to evaluate the resistance of concrete to sulfate attack is according to ASTM C 1012. This methods determines the length change of mortar bars exposed to sulfate solution. This can be used to evaluate the resistance to sulfate attack for Portland cement, blends of Portland cement with pozzolans or slags and blended hydraulic cements.

The exposure regimen according to the standard contains 352 moles of Na_2SO_4 per m^3 which is equivalent to 50 g/L. The apparatus for this test consists of mixer, cube molds, bar molds, comparator, containers and curing tank. The mortar cubes (50 mm) are prepared according to ASTM C109/109M. Mortar bars of size 25 × 25 × 285 mm are used. A set of 6 bars and 21 cubes are prepared and covered with rigid lids, to make it air – tight and are placed in the curing room for approximately 24 hours at 35°C ± 3 °C. The mortar bars are to be stored in limewater until a strength of 20 MPa is obtained. These bars are then immersed in 5% sodium sulfate solution for a period of 6 – 18 months and the length change is being monitored during storage. The pH of the solution should to be maintained between 6.0 and 8.0. The change in length is measured using a comparator (specified as in ASTM C 490) and is calculated using Eq. 11

$$\Delta L = \frac{L_x - L_i}{L_g} \times 100 \qquad \text{…Eq. 11}$$

Where,

ΔL = change in length at x age, %,

L_x = comparator reading of specimen at x age—reference bar comparator reading at x age, and

L_i = initial comparator reading of specimen-reference bar comparator reading, at the same time

L_g = nominal gage length, or 250 mm (10 in.) as applicable.

Tolerance limits for various cement types is specified in the standard. For a test to be valid at a particular age data from a minimum of three bars is required. The maximum permissible range must not exceed the values of change in length in percent corresponding to the number of specimens that are remaining as listed in Table 1.

Table 1: Maximum Permissible Range of Values

Remaining No. of Specimens	**Blended Cements**	**Portland Cement**
3	0.034	0.010
4	0.037	0.011
5	0.039	0.012
6	0.041	0.013

The existing test method to evaluate concrete resistance to sulfates attack has much criticism but is the only standardized method to determine the performance of various cement types exposed to external sulfates attack. (Hartell 2008) The main drawback of this test is that it has no correlation to field performance. This is because of the small size of the test specimens subjected to the

sulfate concentration, type of sulfate used (sodium sulfate used in laboratories) and complete submersion which has no effect of wetting and drying cycles. The main contribution of this drawback is due to the high sulfate concentration levels (5% Na_2SO_4) which are not usually encountered in field conditions (Drimalas and Lowe 2011).

2.3.3.2 Physical Testing Methods

Evaluation of the degree of deterioration due to sulfates attack can be done using traditional physical testing such as visual grading (Stark 2002), expansion measurement (Kurtis et al. 2000; Monteiro 2006; Monteiro and Kurtis 2003) and loss of mass was also used as a measure to quantify degradation (Haynes et al. 2008).

Stark 1989 proposed visual evaluation of concrete subjected to sulfate exposure. Three concrete specimen types were made:

1) beams of size 6 × 6 × 30 which were placed in sulfate rich soils,
2) cylinders of size 6 × 12 for compressive strength evaluation after 28 days of moist curing
3) Prisms of size 3 × 3 × 11-1/4 to evaluate sulfate resistance in laboratory conditions.

The soil contained about 5.6% sulfate ion by weight of soil. The beams were placed in the soil such that they were buried up to 3 in. To induce crystallization of sulfate salts, periodic flooding followed by atmospheric drying was performed (wetting and drying cycles). Linseed oil and epoxy was used on a few specimens as a protective coating against sulfate attack. A numerical rating system on a scale of 1 to 5 was used to evaluate the concrete specimens. These ratings were established by the California Department of Transportation and Construction Technology Laboratories, Inc. (CTL). It was found that the performance of concrete against sulfate attack

increased as the w/c ratio decreased. For a particular water to total cementitious material, concrete made of only portland cement showed higher resistance than granulated blast furnace slag or fly ash which were used in partial replacements of Portland cement. Higher the slag content lesser was the resistance to sulfate attack. It was also found that the coatings helped in delaying the process and was of no use for mixtures with high w/c. This method suggested that the laboratory testing carried out by immersing the specimens should be evaluated with the effects of wetting and drying cycles. Since this is a visual inspection it can just be considered for a preliminary investigation (Stark 1989). Thereafter, Stark (2002) conducted a long-term study on partially immersed specimens, initiated by the Portland Cement Association, which showed similar results to that of his previous investigations on completely immersed specimens. (Stark 1984, 1989) Based solely on visual inspection, salt crystallization was considered to be the primary damaging mechanism (Stark 1984, 1989).

To understand the deterioration mechanism non-accelerated experimental tests are of great importance. Based on 40-year-old specimens, Monteiro (2006) demonstrated that the scaling laws could be established for porous concrete and the scaling exponent depends on cement composition and not on the water-to-cement ratio. This work developed expansion laws from the most comprehensive experimental methods undertaken. Various concrete mixture designs were selected to evaluate the effect of water to cement ratio, curing temperature, cement composition and admixtures on the expansion of cylindrical specimens exposed to realistic field conditions. For these concrete mixtures, an index of potential for damage was defined, which was strongly correlated with the initiation time. During the 40 year period, the specimens do not show the stage at which the scaling law was applicable as the dense specimens exhibited cyclic saturation curves.

The proposed model may be used to predict the life of existing structures and to predict the characteristics of the reactions which cause “damage/repair” and long-dormant periods where cracks occur and “heal”. This would give the knowledge to find the mixture combinations that will be more suitable for these aggressive conditions (Monteiro 2006).

An accelerated version of the expansive mortar bar test was proposed by NIST researchers (Ferraris et al. 2005). By decreasing the sample size, to increase the exposure surface-to-volume ratio, results were obtained in weeks rather than in months. This procedure was developed from insights provided by petrographic analysis of specimens degraded by sulfate exposure over a period of time. This test uses specimens smaller than those specified in ASTM C 1012. The proposed method gives results similar to ASTM C 1012 but requires less than one third the time, due to the reduction in cross section and protective ends. Comparison of the results of smaller specimens with those obtained from the larger specimens (ASTM C 1012) was also carried out in this study. A length change comparator was also used to measure the expansion. It was observed that the mortar specimens showed greater expansion than cement paste and this may be due to faster penetration of sulfates through the mortar which is more permeable (Ferraris et al 2005).

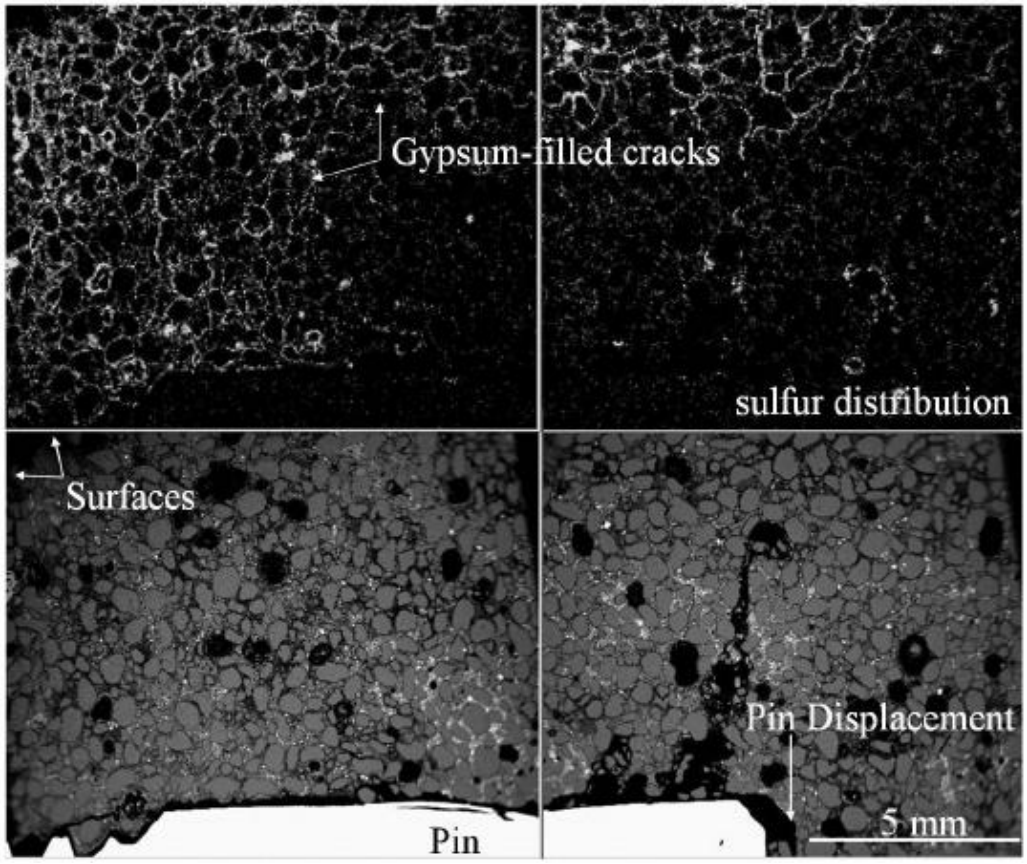

Figure 13: Composite image with about 12 mm total field width with the backscattered electron image of the mortar and end pin (bright rod) and above x-ray images of sulfur highlighting gypsum-filled cracks in the mortar.

(Ferraris et al. 2005).

According to the standard test method, the length change measured is based on the entire volumetric change of the prismatic specimen; however, Ferraris et al. 2005 showed that the tri-dimensional ingress front at the end of the prism possibly affects the results precipitately. The pins may be dislocated and the accuracy of the measurement is disturbed because of the increase

in reactivity at the prism ends and pin tips (Figure 13). In this accelerated mortar bar test the formation of sulfate products results in stresses at the pin ends thus dislodging them affecting the length reading.

2.3.3.3 Strength Testing Methods

Loss in engineering properties of concrete exposed to external sulfates attack can be measured using mechanical testing's such as compressive or tensile strength testing. (Figg 1999; Irassar et al. 1996) Cohen and Mather (1991) stated that the concentration level changes the mechanism of attack which in turn alters the end products. It was also shown that the size and shape of the specimen may affect the reaction kinetics since the increase in surface reaction accelerates the attack mechanism (Cohen and Mather 1991).

Monteiro et al. (2000) proposed an accelerated test method for the evaluation of cement resistance to external sulfates (Caltrans LLPRS Program, California DOT). It is based on the loss in compressive strength of 12.7 mm mortar cubes subjected to external sulfates. The dimension was selected to maximize the surface-to-volume ratio to increase the ingress of sulfate ions into the specimen. Five different cement types were evaluated which were categorized into 3 categories: Portland cements and blends (PC), calcium aluminate cements and blends (CA), and calcium sulfoaluminate cements (CSA). The w/c ratio used was 0.50. The specimens were cured for 7 days and the compressive strength was determined prior to sulfate exposure. The sulfate solution used was 4% Na_2SO_4 that was maintained at a pH of 7.2. The compressive strength was measured at 28 and 63 days and compared to the 7-day control strength. The change in compressive strength was calculated using Eq. 12. (Monteiro et al. 2000)

$$\Delta f(\%) = \frac{f_{xd} - f_{7d}}{f_{7d}} \text{ x } 100 \qquad \text{…Eq. 12}$$

Where,

Δf (%) = Change in strength

f_{xd} = Strength at 28 or 63 days

f_{7d} = Strength at 7 days

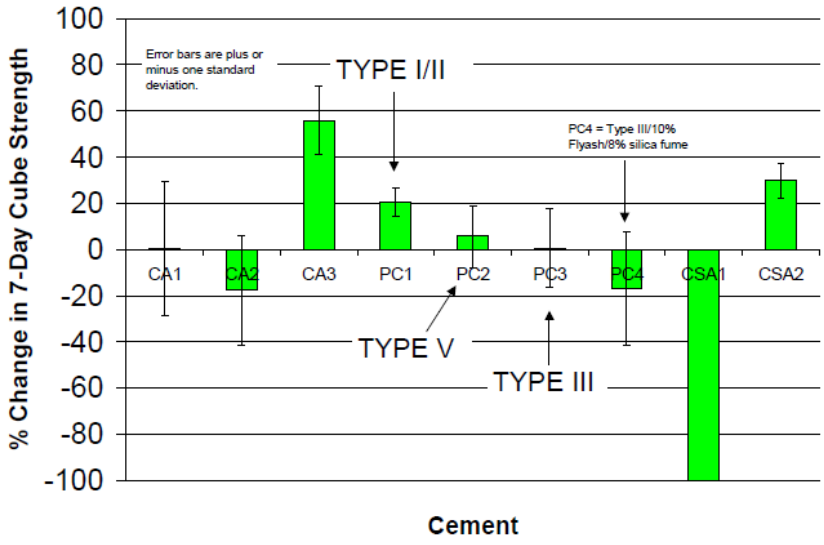

Figure 14: Results of accelerated sulfate test after 4 weeks (28 days) of exposure. Change in strength is based upon strength measured at 7 days of age, prior to exposure, for each cement.

(Monteiro 2006)

It was shown that if the change in strength decreased by 25% the cement was not considered to be sulfate resistant. Loss in strength can be used as an interpretation for the susceptibility to sulfate

attack. The loss of strength may be due to expansive stresses, gypsum and ettringite formation and disintegration of C-S-H. Increase in strength was also observed for certain specimens as they were hydrated in sulfate solution. Figure 14 showed the effect of sulfate attack on the 28 days the compressive strength when compared to 7 day's strength of hydration. At the end of 28 days sulfate exposure, it was found that there was a reduction in strength for three cements. It was noticed that there was a moderate decline in strength of CA2 (Calcium aluminate cements and blends) and PC4 (Portland cements and blends) specimens. CSA1 (Calcium sulfoaluminate cement) specimens had deteriorated to such an extent that they could not be tested for compression. Similar sulfate resistance was observed in Type I/II, Type III, and Type V. (Monteiro 2006)

But, there is a disagreement in considering compressive strength to evaluate the extent of damage when compared to rate of change of tensile strength versus rate of change in compressive strength. (Neville 2004) (Boyd and Mindess 2004)

In Boyd and Mindess, 2004, concrete specimens were partially immersed for different time periods up to 1 year in a sulfate solution. The specimens were prepared with a w/c ratio of 0.45 and 0.65 using ordinary and sulfate resistant cement. Compressive strength and tensile strength tests were used to evaluate the performance of concrete. The tensile strength was measured using the pressure tension test. It was found that the w/c had a greater effect on the resistance to sulfate attack rather than the type of cement. In order to detect the internal damage especially at early ages, the pressure tension test was found to be more sensitive than the compressive strength test. It was found that when concrete is subjected to sulfate attack, the tensile strength of concrete reduces more rapidly than the compressive strength because the tensile strength is more sensitive

to cracking. This suggests that the tensile strength test is more suitable to detect and evaluate expansive damage in concrete (Boyd and Mindess 2004).

2.3.3.4 Nondestructive Testing Methods

Nondestructive testing (NDT) methods are now gaining popularity for their various advantages in measuring the bulk properties and overall nature of the material, for comparative quality assessment of the overall section, quick procedure and for being cost effective.

A study was carried out to investigate the effect on surface wave velocity and through wave velocity when concrete is exposed to sulfate solutions (Scott et al., 2006). For this purpose, the impact-echo method and the ultrasonic pulse velocity test were used. The specimens consisted of 900 × 240 × 485 mm concrete blocks that were immersed in 5% Na_2So_4 for a depth of 150 mm. In order to create a two dimensional exposure condition, the blocks were sealed with epoxy at the ends. Similar control specimens were cast and immersed in saturated limewater. The blocks were evaluated using the ultrasonic pulse velocity and impact - echo after one year exposure period. Three modes of destructive testing: 1) Compressive strength as per ASTM C39. 2) Splitting tensile strength as per ASTM C496. 3) Pressure tensile strength was carried out. The nondestructive data was correlated with the destructive test results for field samples that were continuously exposed to sulfate attack using best fit lines. Previous studies have shown that tension tests on concrete are more sensitive than compressive strength test to such damage. As such, it was found that the wave velocities from the two techniques mentioned correlate better with the tensile strength of concrete than with the compressive strength (Figure 15 – Figure 18). Also, the impact echo method correlated better for predicting the pressure tensile strength than

the ultrasonic pulse velocity for specimens damaged due to sulfate attack. The S-wave speeds from impact echo were lower than the wave speeds from ultrasonic pulse velocity test which indicates that the concrete at surface is more damaged which may suggest that sulfate attack is a surface damage mechanism (Scott et al., 2006).

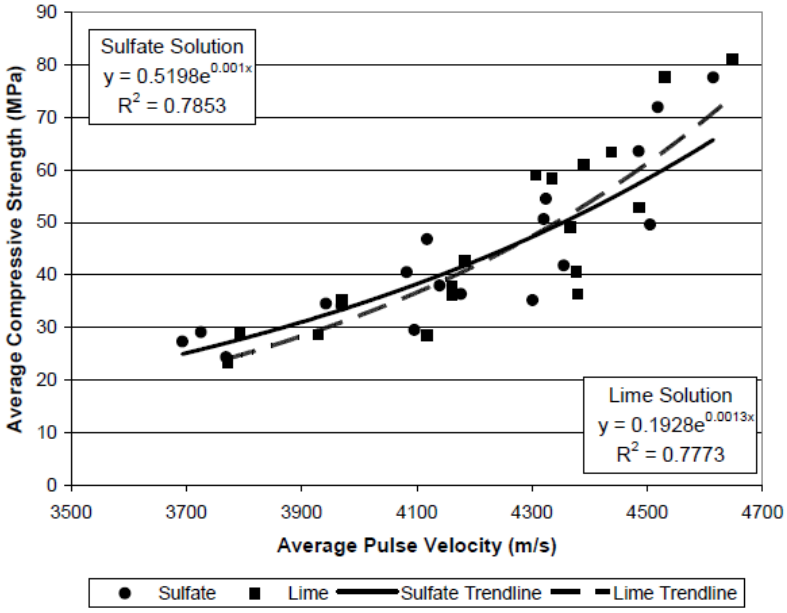

Figure 15: Compressive strength versus P-wave velocity from UPV testing

(Scott et al., 2006).

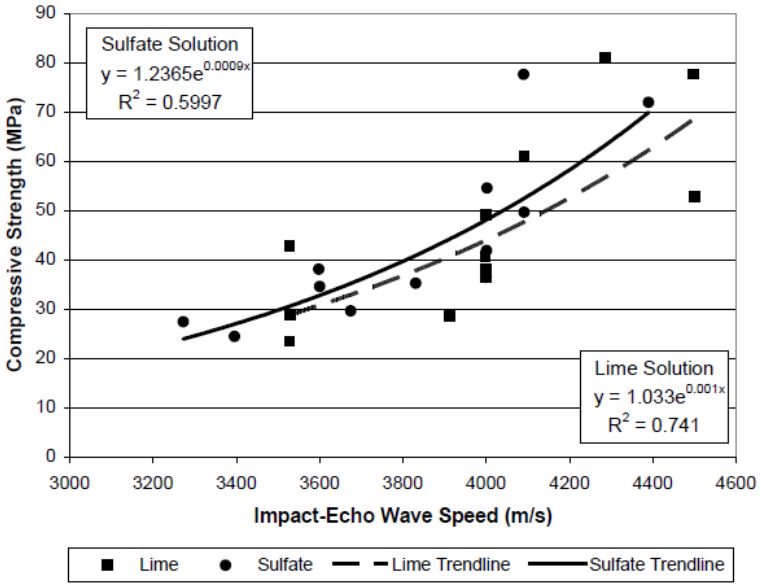

Figure 16: Compressive strength versus surface wave velocity from impact-echo testing.

(Scott et al., 2006).

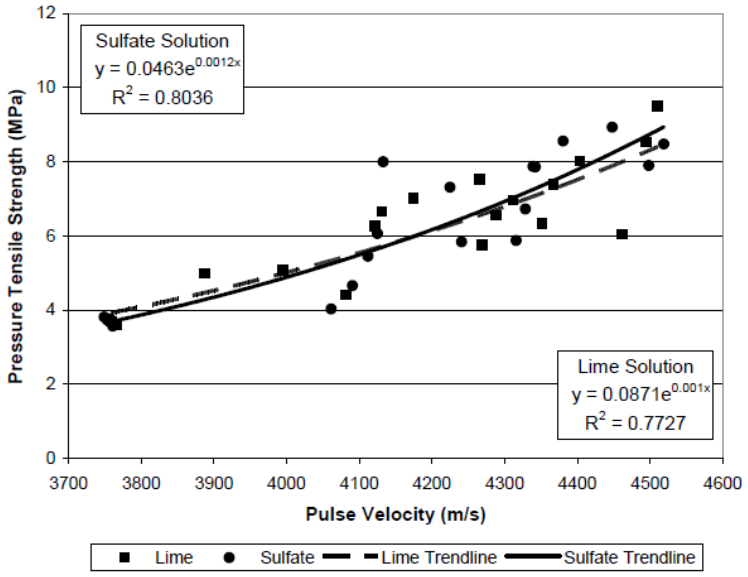

Figure 17: Pressure tensile strength versus P-wave velocity from UPV testing

(Scott et al., 2006).

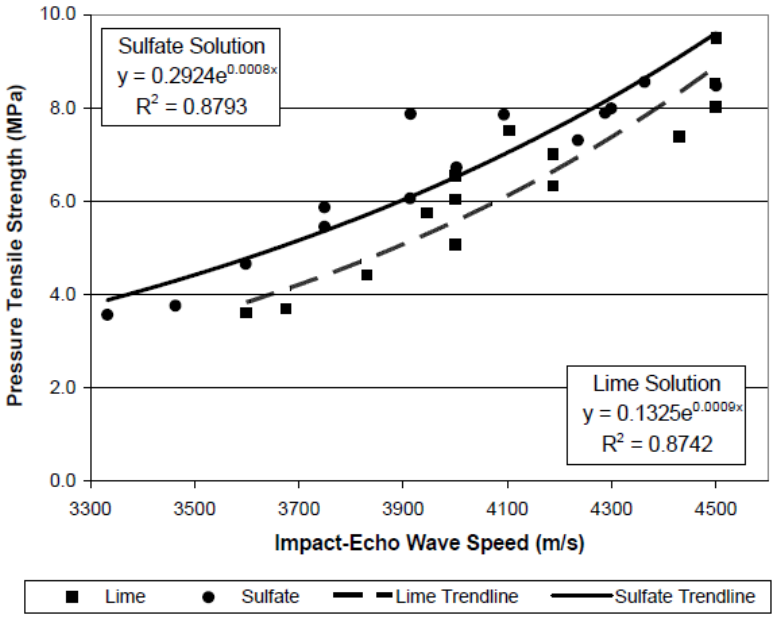

Figure 18: Pressure tensile strength versus surface wave velocity from impact-echo testing (Scott et al., 2006).

A similar experimental procedure was used by Rozière et al. (2009) with resonant frequency which showed reliable results at the early detection of sulfate distress. But, the results from these tests is dependent on the physical condition of the specimen and thus a decrease in accuracy of the results is observed as the extent of deterioration increases. (Whitehurst 1966). Therefore, ultrasonic testing may be a viable form of testing for assessing sulfate related degradation mechanisms; this study proposes a methodology to further investigate its potential in evaluating the effects of sulfate exposure.

CHAPTER 3

EXPERIMENTAL METHODOLOGY

To measure the degradation and loss in properties of concrete, appropriate test methods have to be used. In this study, the loss of attenuation due to damage through the bulk of the material is studied to determine whether ultrasonic measurements may be a useful tool to evaluate sulfate damage.

3.1 Sample preparation

The below sections describe about the specimen preparation and conditioning prior to testing. The materials being used, quality control, curing conditions are being discussed further.

3.1.1 Materials

Aggregates: The specimens were prepared with coarse and fine aggregate which satisfy ASTM C 33 Standard. The coarse and fine aggregates were granite rock from St-Hippolyte, QC, quarry for its low reactivity to chemical attack (Kosmatka et al. 2002) and was donated by Bauval.

Binder: Portland cement of Type GU (general use hydraulic cement) was used according to Canadian specification CAN/CSA-A3000-08. This cement type was chosen over sulfate resistance cement in order to accelerate the degradation mechanism due to sulfate attack. The cement used was donated by Lafarge and was manufactured at St-Constant, QC, cement plant.

Water: Tap water from city supply of Montreal, QC. No quality testing was carried out as the water source was considered potable.

Admixtures: A set retarder was used in order to increase the initial set time. This helped in casting and finishing over 100 samples within an acceptable time limit (before initial set). This also helped in increasing the workability as the fluidity of concrete is increased. Daratard 17, donated by Grace Construction Products, Lasalle, Quebec was used. To set the initial set time by 2 hours, a dosage of 195 ml per 100 kg was chosen.

3.1.2 Mixing and Casting

The objective of this study was not to analyze the effects of concrete mixture parameters or cement composition but to evaluate the wave attenuation over a period of time when the concrete is exposed to various exposure conditions. The mix design was calculated using Cement Association of Canada guidelines, *Design and Control of Concrete Mixtures, 7th Ed.* The water to cement ratio chosen for this study was 0.48, according to ASTM C 1012. The water to cement ratio chosen yields a compressive strength of 35Mpa. The mixing was done according to ASTM C172 international standard.

Casting was done according to ASTM C 192 / C 192 M standard. Moisture correction was considered for the determination of water content. The casting was done under the controlled environment of McGill's construction materials laboratory facilities and fresh properties of concrete i.e., slump, air content were verified for every batch.

- Slump : This test was carried out according to ASTM C 143/ C 143M standard and is used to find the consistency of concrete

- Air Content: This test was carried out according to ASTM C 231/ C 231M standard.

The values designed for air content was 2.5 % and 60 mm for the slump (140 mm after admixture being added). The measured values were within ± 10% between the batches. The mix design of the concrete is described in Table 2. In Hartell 2014, several hundred specimens were prepared and subjected to various exposure regimens and test methods; however, for the purpose of this investigation, only one type of specimen is considered: ⌀ 100 mm × 200 mm cylindrical specimens completely immersed in solution for periods of 3, 6, 12, 18 and 24 months. A total of 6 replicates (3 controls and 3 sulfates) were prepared from the same batch of materials for each exposure age. Each batch was prepared at different times over a 2-year period. They were compacted in two equal layers using external vibration to consolidate into cylindrical molds.

Table 2: Mix Design Calculations

Material	**Type**	**Quantity**	**Units**
Cement	GU	448.18	Kg/m^3
Coarse Aggregate	5-14 mm, Granitic rock, St-Hippolyte quarry (dry)	848.00	Kg/m^3
Fine Aggregate	0-5 mm, Granitic rock, St-Hippolyte quarry (dry)	838.00	Kg/m^3
Water / Cement		0.48	-
Water	Potable, City of Montreal	217.45	Kg/m^3
Admixture	Daratard 17, Grace	872.73	ml

3.1.3 Specimen Curing and Conditioning

After the initial set, the samples were covered under a loosely sealed wet burlap under a plastic tarp for 24 hours. The specimens were demolded and stored in the laboratory for 7 days under ambient conditions, 20 ± 1.5^{0}C and 50% RH. Further curing was not carried out in order to represent field conditions (Hartell et al. 2012; Boyd and Mindess 2004). During this time, the end surfaces of the specimens were painted with three layers of epoxy coating (Sikadur 32 Hi-mod) to seal them. This procedure was followed in order to prevent a tri-dimensional ingress front and prematurely degrade the specimen ends (Hartell 2014). As mentioned in section 2.3.3.2, according to the standard test method, the length change measured is based on entire volumetric change of prismatic specimen. But, Ferraris et al. 2005 showed that the tri-dimensional ingress front at the end of the prism possibly affects the results precipitately.

As known, exposure conditions and the amount or concentration of sulfate solution the concrete is exposed will have physical and chemical adverse effects on the material. However, for the purpose of this study, only one sulfate transport mechanism will be investigated: the standard diffusion-based transport mechanism. The cylindrical specimens were submerged (Figure 19) in two different solutions: a 5% sodium sulfate solution as recommended in the ASTM C1012 standard and a lime-saturated solution was used for the control specimens to prevent leaching. The samples were exposed to their respective solutions for periods of 3 months, 6 months, 12 months, 18 months and 24 months (Hartell 2014).

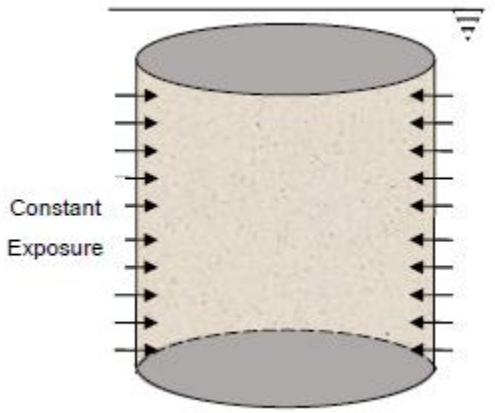

Figure 19: Bi-dimensional diffusion transport mechanisms for cylinder samples

(Hartell 2014)

3.2 Testing Methods

This section describes the ultrasonic pulse emission test procedure performed to evaluate the wave propagation properties of the affected concrete. Standard cylindrical specimens were used for evaluating both wave velocity and wave attenuation through a cementitious matrix in order to evaluate the extent of damage along its travel path.

3.2.1 300 kHz Diametrical Ultrasonic Pulse Emission Test

Hartell (2014) developed a test procedure to assess the extent of sulfate damage by comparing the change in velocity of an ultrasonic pulse over the height of cylindrical specimens. Damage profiles were created for all cylindrical specimens. These were used to evaluate the extent of damage. The procedure carried out was according to the principles of ASTM C597 standard.

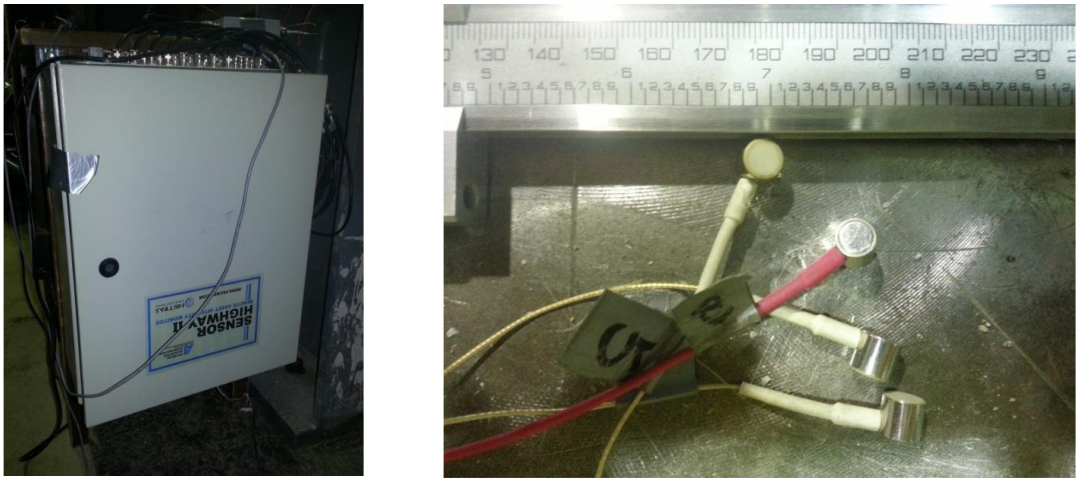

(a) (b)

Figure 20: a) Highway II AE system and, b) Nano30 sensors.

(Hartell 2014)

A Highway II acoustic emission monitoring system from Physical Acoustics Corporation was used to perform the test (Figure 20 a). A miniature resonant sensor called Nano30 with high sensitivity was used to glue on to the circular surface, these sensors were chosen as they are small and they do not lose the contact (Figure 20 b) (Hartell 2014). The capability of the sensor to pulse made it feasible to use the Automatic Sensor Test (AST) an integrated feature in AEWIN, an AE system's operating software. The emitting sensor emits an ultrasonic pulse and the receiver records all parameters of the wave during an AST test (Hartell 2014).

As seen in Figure 5, sensors at every 25mm (for the entire length of the specimen) were glued on the circular surface with a hot glue. The sensors were glued at 90 degrees to each other and readings were noted across the diametrical axes. The required wave parameters were stored in data files of file type, .DTA. The wave parameters considered for this study were travel time and amplitude (Hartell 2014). The diameter dimensions at every 25mm was measured to calculate the

velocity and the amplitude attenuation (Figure 21). Equation 7, presented in section 2.2 was used to calculate the wave velocity across the diametral axis. The attenuation or loss in signal strength was calculated using the following equation (Eq. 13) based on equation 8 presented in Section 2.2.1:

$$\alpha = \frac{(A_0 - A_x)}{x} \quad \text{… Eq. 13}$$

Where,

A_0 = initial amplitude (99 dB)

A_x = amplitude travelled after x distance (dB)

x = distance travelled (distance between sensors) (mm)

α = attenuation coefficient (dB/mm)

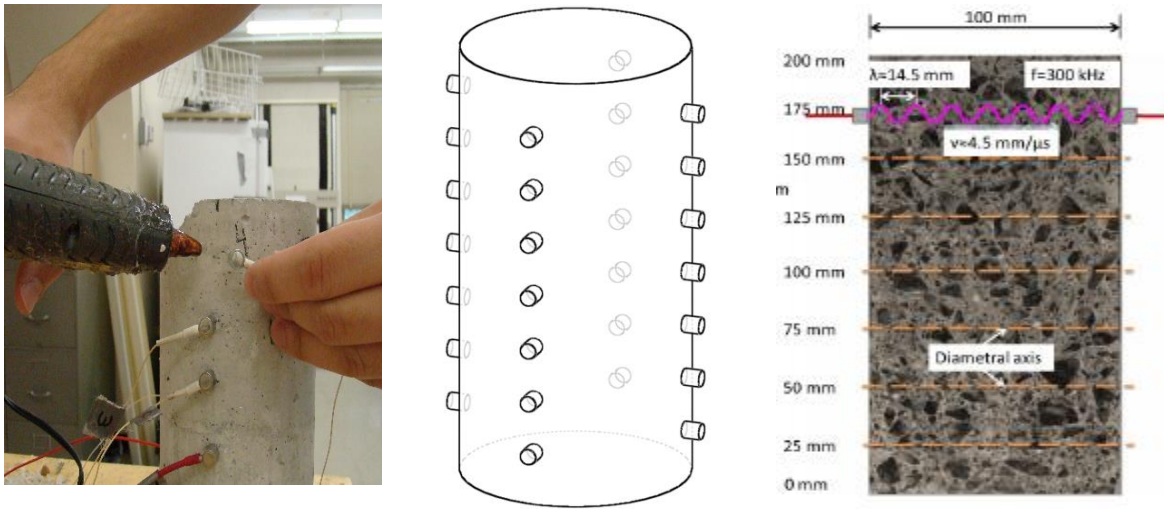

(a) (b) (c)

Figure 21: (a) Diametral ultrasonic pulse emission test, (b) Graphical representation of the sensor placement, (c) UPV test locations and properties of 300 kHz Diametral ultrasonic wave.

It is important to mention that the specimens were tested in saturated conditions to ensure good results as for the specimens in dry condition the difference in acoustic impedance between concrete and air in the voids is too large and the wave would not be able to travel through it, causing greater attenuation of the ultrasonic wave. The specimens were immersed in potable lime water for 5 ± 0.5 days before the tests were carried out. All tests were carried out in a controlled environment within the Construction Materials laboratory at McGill University, Montreal, Quebec. (Hartell 2014)

CHAPTER 4

RESULTS AND DISCUSSIONS

A number of physical and chemical reactions occur when concrete is exposed to external sulfates. This causes deterioration of concrete and changes in mechanical properties. Therefore, it is important to develop appropriate means to assess the loss in integrity based on current understanding of the mechanism of sulfate attack. This study evaluates the effectiveness of ultrasonic through transmission testing method as means to assess the behavior of concrete under sulfate attack. All measurements taken and calculated velocity and attenuation, based on the recorded travel time and amplitude of the received ultrasonic pulse (section 3.2), are detailed in Appendix A.

To evaluate the possibility of a correlation between both parameters in the presence of a degradation mechanism, velocity versus attenuation figures were prepared and a regression analysis was conducted. Thereafter, to evaluate the effectiveness of both parameters to assess any changes due to sulfate ingress, a statistical analysis was performed. The average and the standard deviation were calculated for specimens in limewater and 5% sodium sulfate solution for each exposure period. Again, all results are presented in Appendix A and plotted in the figures below.

Then, to help in the analysis, the coefficient of variations were calculated using the following Eq. 14

$$S^2\ (\%) = \frac{S}{\mu} \times 100 \qquad \ldots \text{Eq. 14}$$

Where,

S^2 = Coefficient of Variance

S = Standard Deviation

μ = Mean of all the values

Moreover, an F-test and a T-test were carried out to statistically determine whether the results obtained were statistically similar or distinct. F - Test was used to find out if the two sets of data have the same variance or unequal variance. If the probability returned is < 0.05, the sets are meant to have equal variance and if it is > 0.05, the sets are said to have unequal variance. Depending whether the data sets had equal or unequal variance, the T - Test values were computed. If the probability returned is < 0.05, it is said that the data was distinct and vice - versa. These statistically computations were carried out between velocities of limewater (LW) and velocities of 5% sodium sulfate (SS5) specimens for each exposure period. The same was carried out for statistical determination of wave attenuation.

Finally, a comparative analysis with other studies such as Monteiro 2006, as mentioned in Section 2.3.5, was performed. To do so, the velocity values recorded during AST were converted into compressive strength values of the concrete cylinders using the following procedure:

As, mentioned in Section 2.1 (Eq. 2), the speed of transient wave can be calculated using Eq. 15 (Pierce 1989),

$$v = \sqrt{\frac{E(1-v)}{\rho(1+v)(1-2v)}} \quad \text{… Eq. 15}$$

Solving the above equation for Young's Modulus produces Eq. 16 (Carmichael 2009),

$$E = \frac{v^2\,(1+\nu)(1-2\nu)\rho}{(1-\nu)} \quad \text{… Eq. 16}$$

Where,

E: Young's modulus

C_p: P wave velocity

ρ: density

v: Poisson's ratio

The empirical relationship between Young's modulus and compressive strength of concrete is given by Eq. 17 (ACI Committee 318),

$$E = 33 w_c^{1.5} \sqrt{f_c} \quad \text{… Eq. 17}$$

Where,

E = Young's Modulus (psi)

w_c = unit weight of concrete (pcf)

f_c = 28 day Compressive strength of Concrete (psi)

The empirical formula for the relation between Young's modulus and compressive strength of concrete was also given as Eq. 18 (Kurtis, http://people.ce.gatech.edu/~kk92/hardconc.pdf)

$$E = 0.043 w_c^{1.5} f_c^{0.5} \quad \text{…Eq.18}$$

Where,

E = Young's Modulus (MPa)

w_c = Density of concrete (kg/m^3)

f_c = 28 day Compressive strength of Concrete (MPa)

Solving Eq.18, compressive strength of concrete can be calculated as the following Eq. 19,

$$f_c = \frac{E}{0.043 w_c^{1.5}} \quad \text{…Eq. 19}$$

4.1 Analysis between Exposure Regimens

As mentioned in section 3.1.4, the specimens were placed in two different concentrations namely, limewater (LW) and 5% sodium sulfate (SS5) for 3, 6, 12, 18 and 24 months. Per specimen type (age and solution exposure), a total of 42 (two diametral measurements at seven heights for three cylinder replicates) velocity vs attenuation measurements are presented on a scattered point plot in the following sections. First, to establish an overall relationship based on material variance, maturity and sulfate exposure alone, all specimen ages are compared with respect to their solution exposure. Then, to better understand the effects of sulfate exposure (without material variance), each specimen age are further analyzed by individually comparing them with their respective controls.

4.1.1 Analysis for Control Limewater Specimens

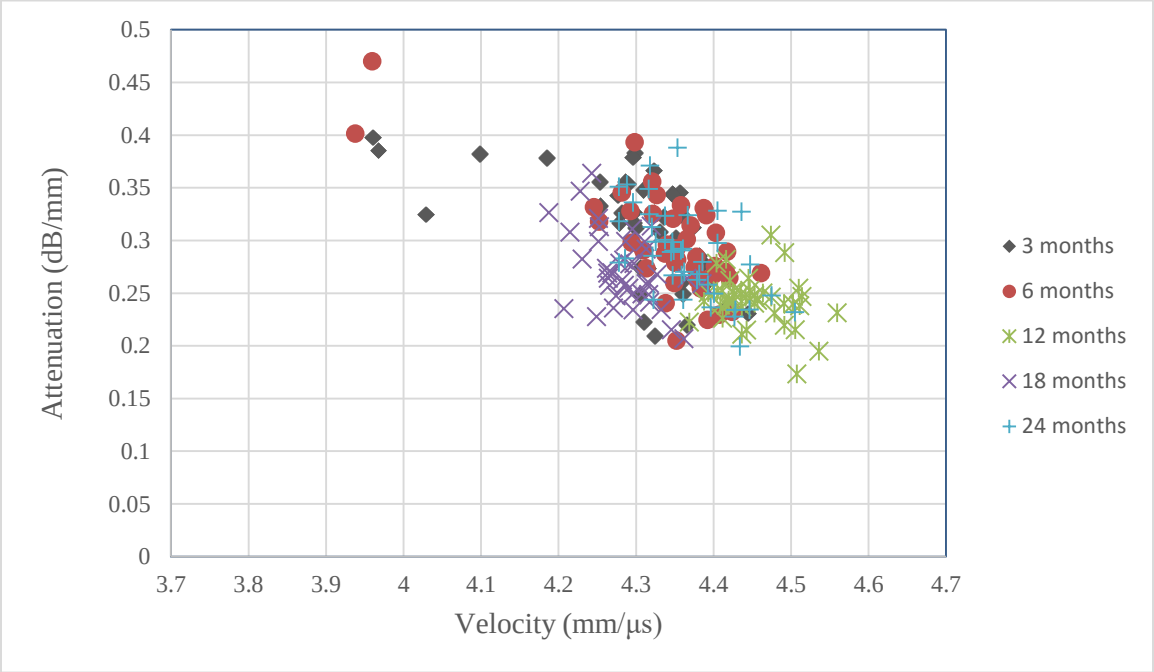

Figure 22: Velocity vs Attenuation for control specimens at 3, 6, 12, 18 and 24 months exposure.

It was noticed that the recorded velocity mainly lies between 4.2 – 4.6 mm/µs with an average coefficient of variation of 1.523% (Refer Section 3.3). The calculated attenuation ranges between 0.2 – 0.4 dB/mm with an average coefficient of variation of 9.585% (Section 3.3). Although the same mixture design was used, each specimen age were batched and mixed on different dates throughout the year. It is well known that the predominant microstructure responsible for mechanical strength is well established after only 3 months of curing time; therefore, specimen maturity should not be a predominant factor in the observed variability. This is observed in figure 22. Here, inherent material variability may be the cause for the observed coefficient of

variation across specimen age and slightly higher velocities observed after only 12-months of curing time. Individually, a specimen type cast from the same batch of materials, the velocity coefficients of variation calculated are 2.122 %, 1.658 %, 0.587 %, 0.807 %, 1.101 % at 3, 6, 12, 18 and 24 months respectively; however, the attenuation remains in the same range of values with attenuation coefficients of variation of 12.849 %, 13.452 %, 7.856 %, 11.133 %, 14.327 % at 3, 6, 12, 18 and 24 months respectively.

4.1.2 Analysis for Degraded Sodium Sulfate Specimens

From the Figure 23, it can be observed that the clusters now show the velocity range in 4.0 – 4.5 mm/μs. The coefficient of variance for the velocity is 1.827 % (calculated according to section 3.3) which was higher than that observed for the control specimens. The calculated attenuation ranges between 0.2 – 0.4 dB/mm with an average coefficient of variation of 9.292% (Section 3.3). This increase in the variance of velocity can be attributed to the changes in wave propagation mode for the specimens exposed to 5% Na_2SO_4. Due to the sulfate exposure, the paste softens thus decreasing the velocity of the wave as it propagates through the specimen. As explained in section 4.1.1, the higher velocities in this exposure condition was observed for specimens at 12 months period. However, there is a drop in wave velocities observed for 18 and 24 months. Same as for the control specimen, the range in attenuation still remains and does not seem to be affected by paste degradation as noticed for the velocity parameter. This may prove the statement from section 2.2.1 by Philippidis and Aggelis (2004) true, i.e., the attenuation is affected mainly by aggregates and sulfates do not degrade aggregates. Individually, a specimen type cast from the same batch of materials, the velocity coefficients of variation calculated are 1.375 %, 1.260 %, 4.358 %, 1.917 %, 1.580 % at 3, 6, 12, 18 and 24 months respectively; however, the attenuation

remains in the same range of values with attenuation coefficients of variation of 10.680 %, 9.428 %, 19.979 %, 14.950 %, 16.151 % at 3, 6, 12, 18 and 24 months respectively.

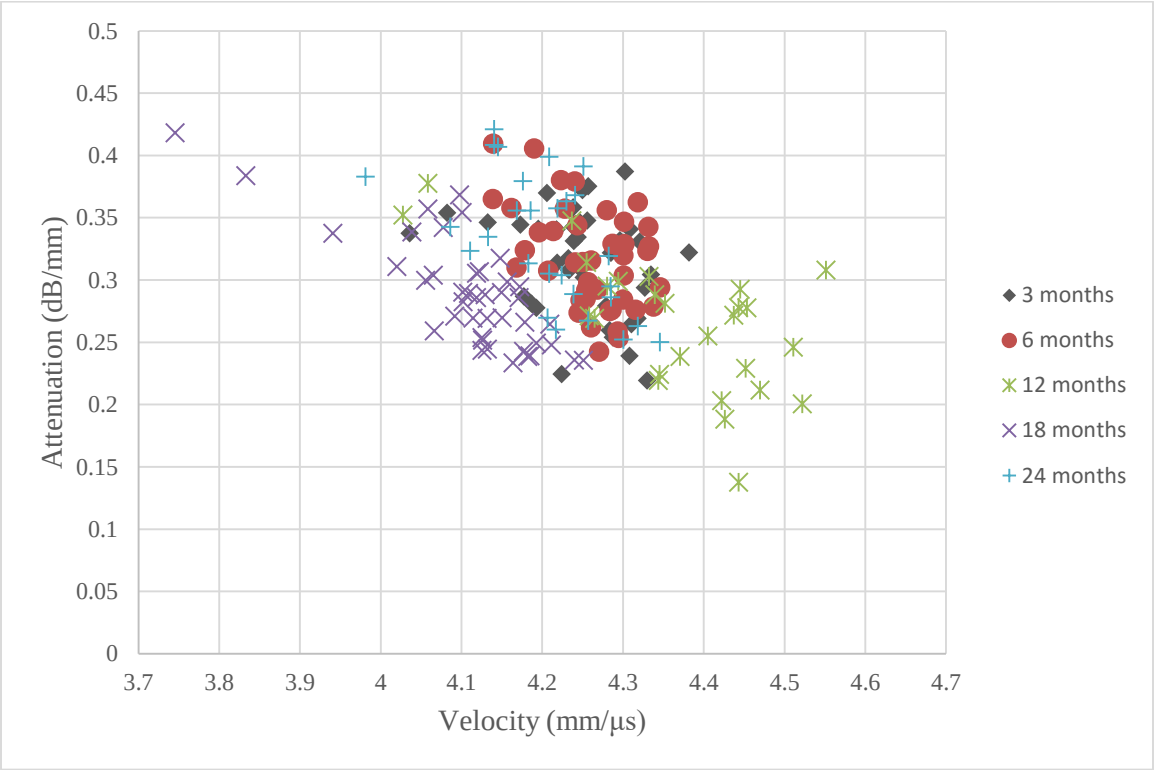

Figure 23: Velocity vs Attenuation for sulfate specimens at 3, 6, 12, 18 and 24 months exposure.

4.2 Comparative Analysis between Specimen Age

A comparative study is made for limewater (LW) and 5% Na_2SO_4 (SS5) exposure for different ages of concrete (i.e., 3, 6, 12, 18 and 24 months).

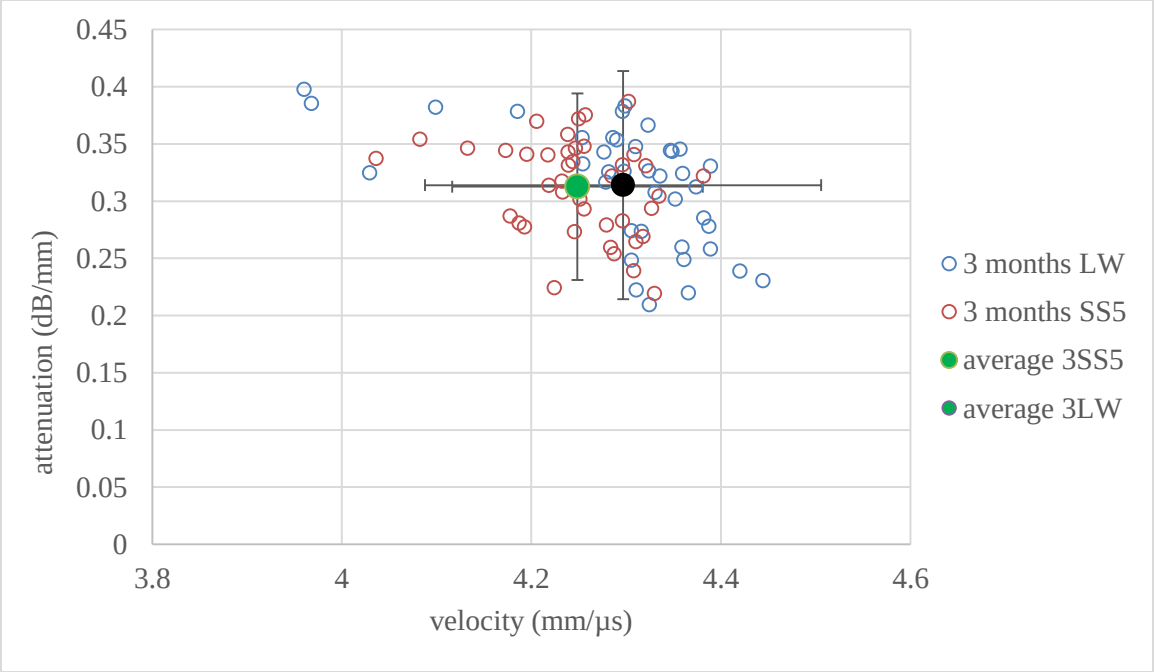

Figure 24: Velocity vs Attenuation for 3 months solution exposure with SSD range

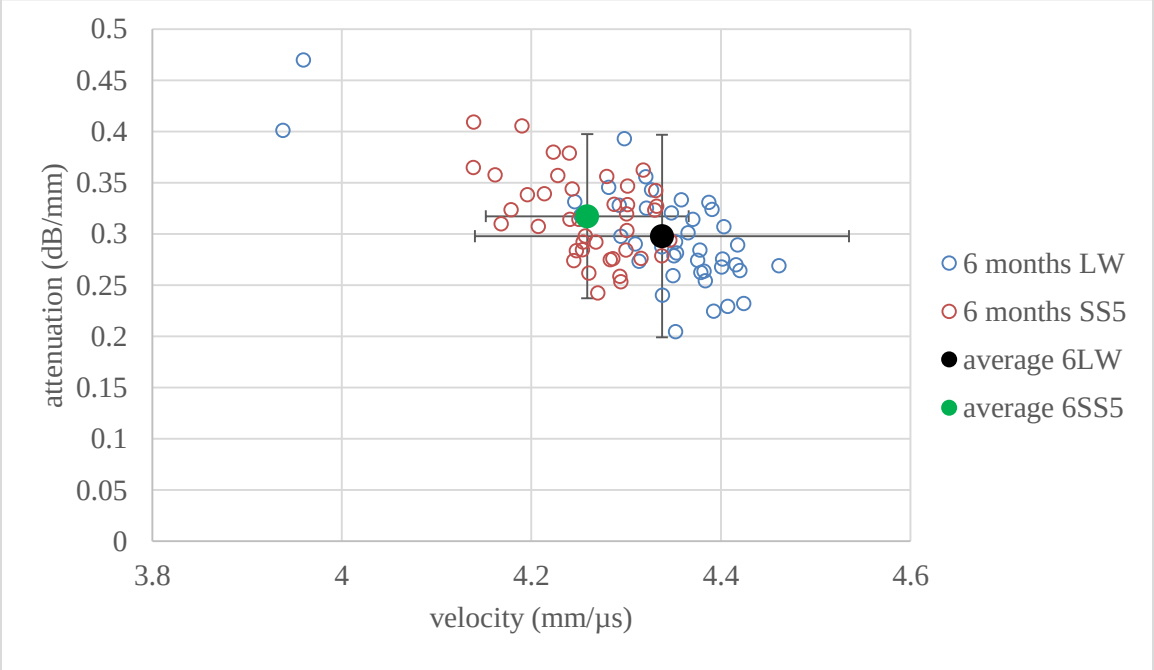

Figure 25: Velocity vs Attenuation for 6 months solution exposure with SSD range.

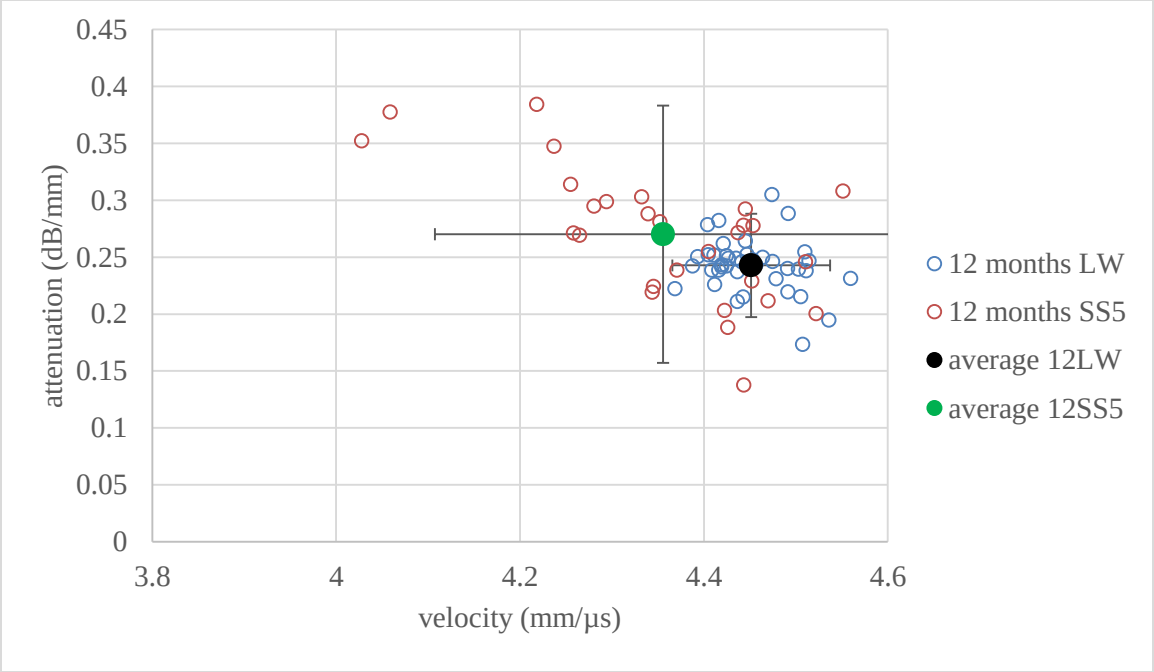

Figure 26: Velocity vs Attenuation for 12 months solution exposure with SSD range

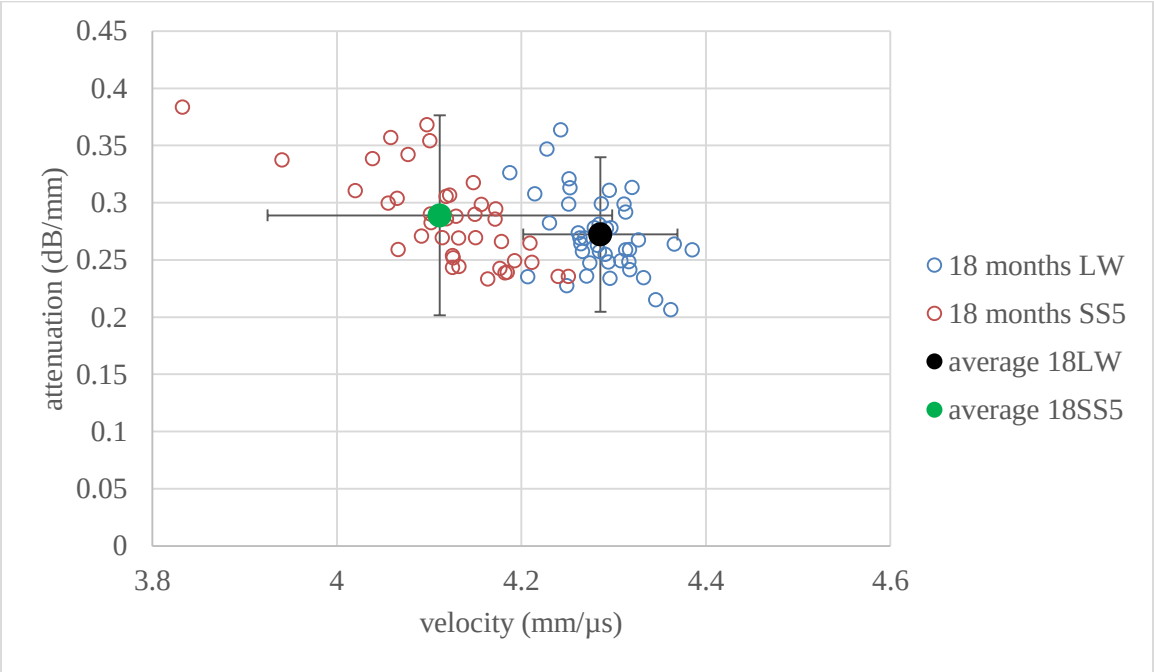

Figure 27: Velocity vs Attenuation for 18 months solution exposure with SSD range

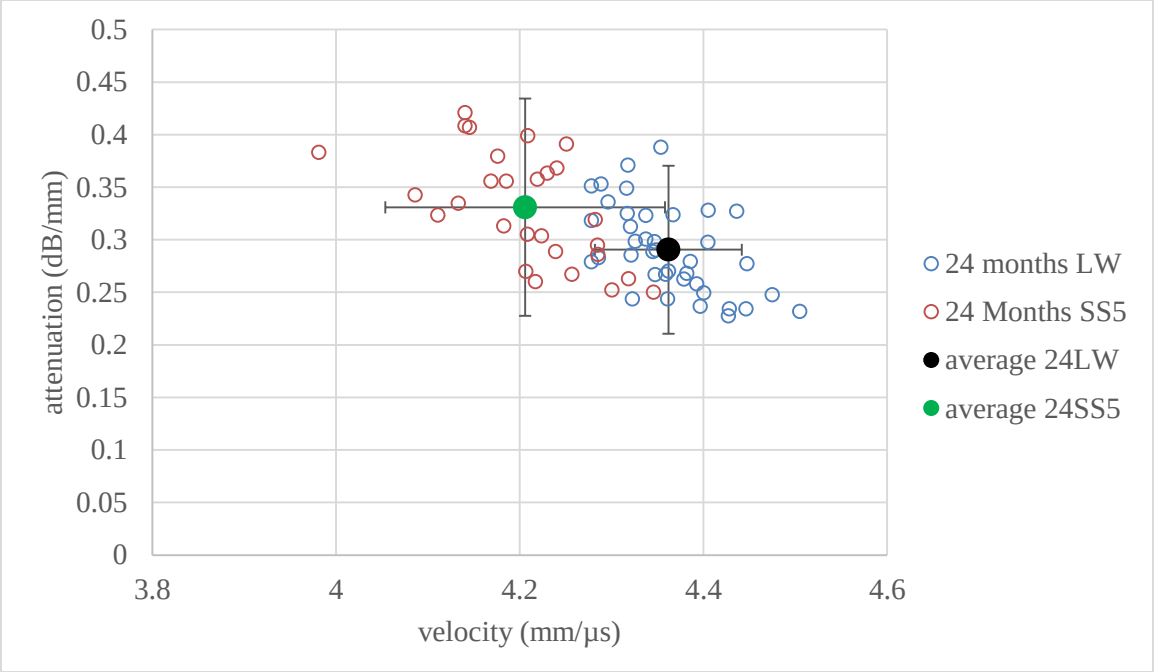

Figure 28: Velocity vs Attenuation for 24 months solution exposure with SSD range

This analysis was carried out to investigate the effects of sulfate exposure on concrete and how sensitive the test method is to assess the degradation mechanisms. It can be observed from Figure 24 to Figure 28, that as the age of the concrete increases, the velocity is decreasing, but the attenuation remains approximately the same. It can also be observed that as the age of the concrete increases intertwining of LW velocity clusters and SS5 velocity clusters decreases (i.e., they become distinct). This demonstrates that with time sulfates degraded or softened the paste enough to change the propagation characteristics of a transient wave. However, the same cannot be concluded when looking at the range in attenuation. Again, as previously discussed, attenuation does not seem to vary due to sulfate exposure.

Philippidis and Aggelis (2004) determined that the degree in attenuation mainly depends on the aggregate structure and not the paste. The density boundaries (paste-aggregate interface) contribute to wave scatter and energy absorption thus attenuating the strength of the transient pulse. Since the granitic aggregate structure remained sound, it may explain the statistically similar results. Therefore, the test could be effective in measuring the extent of an attack on the paste portion of a concrete mixture and the concrete mixture in its entirety.

4.3 Comparative Analysis of Change in Velocity and Change in Attenuation

A graph is plotted with change in velocity versus average attenuation for specimens in SS5 (5% Na_2SO_4) condition (Figure 34). Change in velocity is calculated from the difference in average velocity for limewater and average velocity in SS5 condition for each period of exposure i.e., 3, 6, 12, 18 and 24 months. The F – Test and T - Test was carried out as mentioned at the start of this chapter and is shown in Table 3 and Table 4.

Table 3: F – Test results

F-Test		
Months	**Velocity**	**Attenuation**
3	4.09×10^{-3}	2.03×10^{-1}
6	1.54×10^{-4}	1.80×10^{-1}
12	2.29×10^{-9}	1.90×10^{-7}
18	1.08×10^{-6}	1.04×10^{-1}
24	4.88×10^{-2}	1.29×10^{-1}

Table 4: T – Test results

T-Test		
Months	**Velocity**	**Attenuation**
3	1.47×10^{-2}	8.91×10^{-1}
6	2.98×10^{-5}	5.34×10^{-2}
12	5.28×10^{-4}	2.27×10^{-2}
18	1.52×10^{-15}	5.62×10^{-2}
24	6.82×10^{-12}	6.14×10^{-4}

Table 3 shows F-Test values for velocities and attenuation to demonstrate that there is variance in the spread of the results. Table 4 shows that the values of T - Test for velocities is < 0.05, which means that the data sets are distinct for velocity. The T – Test values for attenuation for 6, 12 and 24 months fall below 0.05, which indicates that these data sets are distinct. But, the T – Test values for 3 months and 18 months for attenuation is greater than 0.05, making the data sets statistically similar.

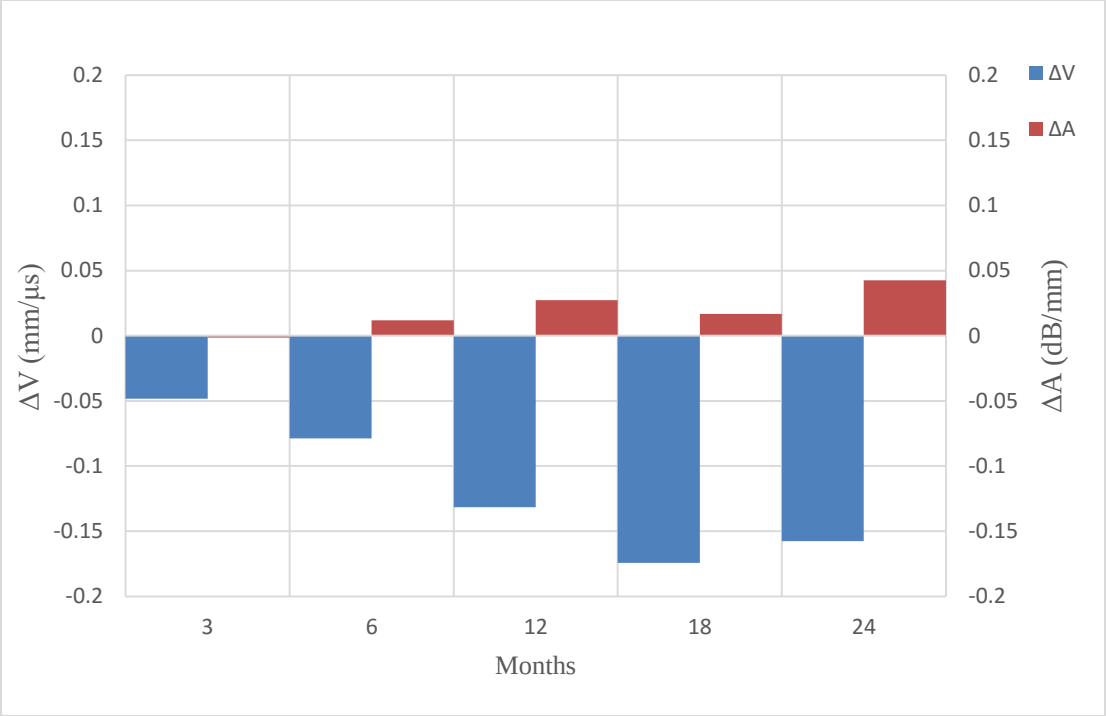

Figure 29: Comparative analysis of change in velocity and change in attenuation

As shown in Figure 29, the change in average velocity between limewater and SS5 has increased as the age of the immersed specimens increased. It can be also observed that there was a negative increase in change in velocity. This is due to the diminishing velocities of the ultrasonic waves through the specimens immersed in SS5 solution, which suggests that the paste is affected. There is also a positive change in attenuation, which indicates that there is an increase in attenuation. But, the increase in attenuation is very much negligible when compared to change in velocities. This supports the previous statement in section 4.1 and section 4.2, that the sulfates do not degrade the aggregates and therefore there is no change in attenuation.

4.4 Compressive Strength Analysis

In order to compare results obtained with previous works on alternative test methods to assess loss in binder properties due to sulfate exposure, the velocity measurement were converted into compressive strength using Eq. 15 – Eq. 19 presented at the beginning of Chapter 4. The compressive strength at different exposure periods was calculated for limewater specimens and sodium sulfate specimens and results are presented in Table 5. Calculations for compressive strength are presented in Appendices A

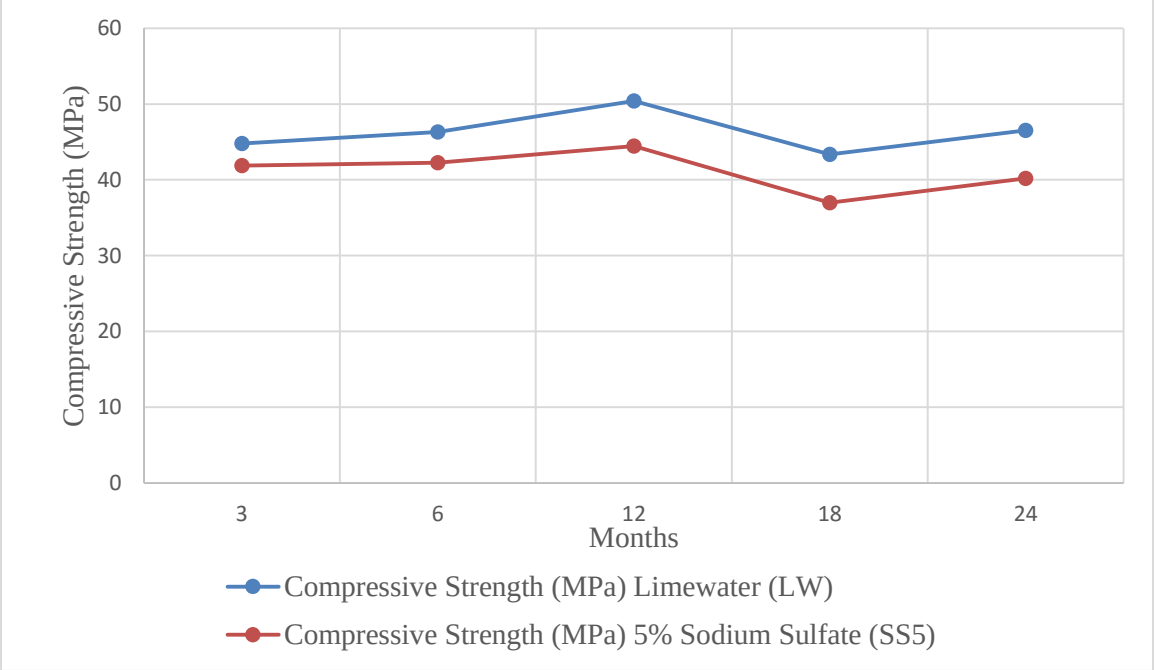

Figure 30: Compressive strength vs age of specimens

It can be observed from Figure 30, that there is a decrease in the compressive strength of sodium sulfate specimens when compared to limewater specimens. As mentioned in the literature review, this may be due to the softening of the cement paste caused by sulfate attack. (Skalny et al. 2002)

As mentioned in the literature review, Monteiro et al. (2006) established that the failure criteria for a sulfate resistance cement was a loss in compressive strength greater than 25 % in comparison to the 7 day compressive strength. Using this criteria, after two years of sulfate exposure, the samples would still satisfy the performance criteria with a loss in strength properties equivalent to 13.6% (Table 5). However, this value is compared to that of the 24-month control.

On-the-other-hand, Hartell (2014) reported that the tested samples actually exhibited a strength gain when subsequently tested under pressure tension. Monteiro (2006) also reported an increase in strength after 28 days of exposure for Portland cement specimens. In Monteiro 2006, the increase in strength was attributed to additional curing time. However, similar conclusions cannot be applied for Hartell 2014 since the curing times were the same for both limewater and sulfate samples. The difference in resulting trend will be further investigated.

Table 5: Compressive strength of specimens at different exposure periods

Months	**Compressive Strength (MPa)**		
	Limewater (LW)	**5% Sodium Sulfate (SS5)**	**% Difference in Compressive Strength**
3	44.781	41.861	-6.521
6	46.311	42.269	-8.727
12	50.385	44.433	-11.811
18	43.342	36.957	-14.731
24	46.507	40.203	-13.555

CHAPTER 5

CONCLUSION

Concrete is a heterogeneous material made of cement, fine and coarse aggregate. Durability of concrete is affected due to various reasons such as, salt attack, leaching, stresses due to loading etc. Sulfate attack decreases the durability of concrete by changing the chemical composition of the paste and also the mechanical properties of concrete (Mishra 2014).

In this study, the effect of sulfate on deterioration of concrete is evaluated with the use of wave parameters such as velocity and attenuation. The velocities for the specimens in limewater (LW) was observed to be in the range of 4.2 – 4.6 mm/μs with a variance of 1.523. And, for those in 5% sodium sulfate was 4.0 – 4.5 mm/μs with a variance of 1.827. This decrease in velocity and increase in variance may be due to sulfate exposure, which causes the paste to soften. But, the attenuation range for both the exposure conditions was observed to the same and was in the range of 0.2 – 0.4 dB/mm. This shows that the attenuation does not seem to be affected by paste degradation as noticed for the velocity parameter (Section 4.1).

It is also observed that as the age of the concrete increases, the velocity decreases and also the velocity clusters for the specimens in LW and SS5 become distinct. This indicates that sulfate exposure may have altered the mechanical and physical properties (i.e. dynamic modulus of elasticity and density) of the paste matrix. Over the time period, it was noticed that the attenuation

coefficient still remains similar, indicating, that attenuation is not affected by the duration of sulfate exposure.

There is a decrease in the compressive strength of sodium sulfate specimens when compared to limewater specimens, this may be due to the softening of the cement paste caused by sulfate attack (Skalny et al. 2002).

In comparison to previous studies suggesting alternate methods, based on mechanical properties, for assessing sulfate resistance of a cement or concrete mixture; ultrasonic testing and the change in velocity values may offer a viable approach. The sensitivity of the method to changes in matrix characteristics is demonstrated herein; thus, the method should be further investigated.

REFERENCES

A.I. Sagaidak and S.V. Elizarov (2006). "Acoustic emission parameters correlated with fracture and deformation processes of concrete members." Construction and Building Materials, 21, 477–482.

ACI 228.2R-13, “Report on Nondestructive Test Methods for Evaluation of Concrete in Structures”. ACI Committee 228, American Concrete Institute. Farmigton Hills, MI, 2013, 86 pp.

Afshin Sadri, Koorosh Mirkhani (2009). "Wave Propagation Concrete NDT Techniques for Evaluation of Structures and Materials." ASPNDE, NDT group, Canada.

ASTM C 1012 (2004). “Standard Test Method for Length Change of Hydraulic-Cement Mortars Exposed to a Sulphate Solution,” ASTM International

ASTM C 143 / C 143 M (2008). “Standard Test Method for Slump of Hydraulic-Cement Concrete.” ASTM International

ASTM C 172 (2008). “Standard Practice for Sampling Freshly Mixed Concrete,” ASTM International

ASTM C 192 (2008). “Standard Practice for Making and Curing Concrete Test Specimens in the Laboratory” ASTM International

ASTM C 192 (2008). “Standard Practice for Making and Curing Concrete Test Specimens in the Laboratory” ASTM International

ASTM C 231 (2010). “Standard Test Method for Air Content of Freshly Mixed Concrete by the Pressure Method,” ASTM International

ASTM C 33 (2012). “Standard Specification for Concrete Aggregates.” ASTM International

ASTM C 490 (2004). “Standard Practice for Use of Apparatus for the Determination of Length Change of Hardened Cement Paste, Mortar, and Concrete” ASTM International

ASTM C 597 – 97 (2009). “Standard Test Method for Pulse Velocity through Concrete” ASTM International

ASTM C109/ C109M (2002). “Standard Test Method for Compressive Strength of Hydraulic Cement Mortars (Using 2-in. or 50-mm Cube Specimens)” ASTM International

Basista, M., and W. Weglewski (2009). “Chemically Assisted Damage of Concrete: A Model of Expansion under External Sulphate Attack.” International Journal of Damage Mechanics, 18,155-175.

Boyd, A.J. and S. Mindess (2004). “The Use of Tension Testing to Investigate the Effect of W/C Ratio and Cement Type on the Resistance of Concrete to Sulphate Attack,” Cement & Concrete Research, 34, 3, 373-377.

CAN/CSA-A23.1-04. Concrete materials and methods of concrete construction. Canadian Standards Association, Mississauga, On.

Cement Association of Canada guidelines, Design and Control of Concrete Mixtures, 7th ed

Cohen, D.M. and B. Mather (1991). “Sulphate Attack on Concrete – Research Needs.” ACI Materials Journal, January-February, 62-69.

D.G. Aggelis, T.P. Philippidis (2004). "Ultrasonic wave dispersion and attenuation in cement mortar." NDT & E International, 37, 617-631.

Dr. Choon B. Park (2007). “seismic waves”. Park seismic. <http://www.parkseismic.com/Whatisseismicwave.html> (July 02, 2015)

Ferraris, Chiara, Paul Stutzman, Max Peltz, and John Winpigler (2005). “Developing a More Rapid Test to Assess Sulphate Resistance of Hydraulic Cements.” Journal of Research of the National Institute of Standards and Technology, 110, 5, 529-540.

Figg, J. (1999). “Field Studies of Sulphate Attack on Concrete” in: Materials Science of Concrete: Sulphate Attack Mechanisms. J. Marchand and J.P. Skalny eds., American Ceramic Society, Westerville OH, 315-323.

Gopal Mishra (2014). “Sulphate attack in concrete”. The constructor. <http://theconstructor.org/concrete/sulphate-attack-in-concrete-and-its-prevention/2162/> (July 10, 2015)

Hartell, J. (2014). “Investigating Various Test Methods for Assessing the Effect of Sulphate Attack on Concrete Properties”. Dissertation, McGill University. Dept. of Civil Engineering and Applied Mechanics. Thesis

Irassar, E.F., A. Di Maio and O.R. Batic (1996). “Sulphate Attack on Concrete with Mineral Admixtures.” Cement and Concrete Research, 26, 1, 113-123.

Kurtis, K.E., P.J.M. Monteiro and S.M. Madanat (2000) “Empirical Models to Predict Concrete Expansion Caused by Sulphate Attack,” ACI Materials Journal, March-April, 156-161.

Kurtis, K.E., P.J.M. Monteiro and S.M. Madanat (2000) “Empirical Models to Predict Concrete Expansion Caused by Sulphate Attack,” ACI Materials Journal, March-April, 156-161.

Mistras group (2013), "Acoustic emission theory", <http://www.mistrasgroup.gr/acoustic_emission_theory_eng.htm> (July 02, 2015)

Monteiro, P.J.M. (2006). “Scaling and Saturation Laws for the Expansion of Concrete Exposed to Sulphate Attack.” Proceedings of the National Academy of Sciences of the United States of America 103, 31, 11467–11472.

Monteiro, P.J.M. and K.E. Kurtis (2003). “Time to Failure for Concrete Exposed to Severe Sulphate Attack.” Cement and Concrete Research, 33, 987–993.

Neville, A.M (2004). “The Confused World of Sulphate Attack on Concrete,” Cement and Concrete Research, 34, 1275–1296.

Nick Winter (2005). “Sulphate Attack in concrete and motor.” Understanding cement. <http://www.understanding-cement.com/sulfate.html)> (July 07 2015)

P.A. Gaydecki, F.M. Burdekin, W. Damaj, D.G. John, P.A. Payne 1992. "The propagation and attenuation of medium-frequency ultrasonic waves in concrete: a signal analytical approach." Measurement Science and Technology, 3, 126–134.

Philippidis, T. P. and D. G. Aggelis (2004). “Experimental study of wave dispersion and attenuation in concrete.” Ultrasonics, 43, 7, 584-595.

Popovics S, Popovics JS (1998). "Ultrasonic testing to determine water–cement ratio for freshly mixed concrete." Cem Concr Aggr, 20, 2, 262–268.

Portland cement Association (2001). "Ettringite Formation and the Performance of Concrete." IS 417.

Rozière, E, A. Loukili, R. El Hachem and F. Grondin (2009). “Durability of concrete exposed to leaching and external sulphate attacks.” Cement and Concrete Research, 39, 1188–1198.

Shigenori Yuyama, Takahisa Okamoto, Mitsuhiro Shigeishi, Masayusu Ohtsu (1994). "Acoustic emission generated in corners of reinforced concrete rigid frame under cyclic loading." Reprinted from Materials evaluation, 53, 3, 409-412.

Shigenori Yuyama, Takahisa Okamoto, Shigeyoshi Nagataki (1992). "Acoustic emission evaluation of structural integrity in repaired reinforced concrete beams." Reprinted from Materials Evaluation, 52, 1, 86-90.

Skalny, J., J. Marchand, and I. Odler (2002). Sulphate Attack on Concrete. Modern Concrete Technology Series, Spon Press, London.

Stark, D.C. (2002). "Performance of Concrete in Sulphate Environments." RD129, Portland cement Association, Skokie, Illinois.

Stark, D.C (1989). Durability of Concrete in Sulphate-Rich Soils. RD097, Portland cement Association, Skokie, Illinois.

T.P. Philippidis, D.G. Aggelis (2004)."Experimental study of wave dispersion and attenuation in concrete." Ultrasonics, 43, 584–595

Tixier, R. and B. Mobasher (2003). "Modeling of damage in cement-based materials subjected to external sulphate attack – part 1: formulation." ASCE Journal of Material Engineering, 15, 4, 305–13.

Whitehurst, E. A (1966). Evaluation of concrete properties from sonic tests. American Concrete Institute, DU

Wong, G.S, and, T. Poole (1988). “Sulphate Resistance of Mortars Using Portland cement and Blends of Portland Cement and Pozzolana or Slag.” Technical Report SL-88-34, US Army Corps of Engineers, Washington, DC.

Chiara Ferraris, Paul Stutzman, Max Peltz and John Winpigler (2005). “Developing a More Rapid Test to Assess Sulfate Resistance of Hydraulic Cements.” J. Res. Natl. Inst. Stand. Technol. 110, 529 – 540.

Paulo J. M. Monteiro, Jeffery Roesler, Kimberly E. Kurtis, John Harvey (2000). “Accelerated Test for Measuring Sulfate Resistance of Hydraulic Cements for Caltrans LLPRS Program”. FHWA/CA/OR-2000/03. University of California, Berkeley

Paul E. Stutzman 2001. “Scanning Electron Microscopy in Concrete Petrography.” National Institute of Standards and Technology, Gaithersburg, Maryland.

Paulo J.M. Monteiro (2006). “Scaling and saturation laws for the expansion of concrete exposed to sulfate attack.” Proc Natl Acad Sci, U S A., 103, 31, 11467–11472.

Neville A. M. (1996). Properties of Concrete, fourth ed., John Wiley and Sons, Inc., New York

Trtnik G., Kavcic F., Turk G., (2009). Prediction of concrete strength using ultrasonic pulse velocity and artificial neural networks Ultrasonics Vol. 49, pp. 53–60.

Z. Ç., Türk K. and Karata M. (2008). Effect of mineral admixtures on the correlation between ultrasonic velocity and compressive strength for self-compacting concrete. Russian Journal of Nondestructive Testing, Vol. 44, No. 5, pp. 367–374.

Castro P. F. and Carino N. J. (1998). Tensile and nondestructive testing of FRP bars. Journal of composites for construction, February, No. 17.

Vipulanandan C. and Garas V. (2008) Electrical resistivity, pulse velocity and compressive properties of carbon fiber reinforced cement mortar. Journal of material in Civil Engineering, pp. 93-101.

Leslie J. R. and Cheeseman W. J. (1949). An ultrasonic method for studying deterioration and cracking in concrete structures. American Concrete Institute Proceedings, Vol. 46, No. 1, pp. 17–36.

Yildirim H., Sengul O. (2011). Modulus of elasticity of substandard and normal concretes. Construction and Building Materials, Vol. 25, pp. 1645–1652

T.H. Panzera, A. L. Christoforo, F. P. Cota, P. H. R. Borges and C. R. Bowen (2011). Advances in Composite Materials - Analysis of Natural and Man-Made Materials: Ultrasonic Pulse Velocity Evaluation of Cementitious Materials. ISBN 978-953-307-449-8.

I. Lawson, K.A. Danso, H.C. Odoi, C.A. Adjei, F.K. Quashie, I.I. Mumuni and I.S. Ibrahim (2011). "Non-Destructive Evaluation of Concrete using Ultrasonic Pulse Velocity." Research Journal of Applied Sciences, Engineering and Technology, 3, 6, 499-504.

Scott R. Cumming, Andrew J. Boyd, Christopher C. Ferraro (2006). "Tensile Strength Prediction in Concrete Using Nondestructive Testing Techniques". Research in nondestructive evaluation, 17, 4.

ASTM C 496 (1996). "Standard Test Method for Splitting Tensile Strength of Cylindrical Concrete Specimens." ASTM International.

Kosmatka, Steven. H., Beatrix Kerkhoff and William C. Panarese (2002). Design and control of concrete mixtures, 14th Ed., Portland Cement Association, Skokie, Illinois, 358 p.

Ulucan Z. Ç., Türk K. and Karata M. (2008). Effect of mineral admixtures on the correlation between ultrasonic velocity and compressive strength for self-

compacting concrete. Russian Journal of Nondestructive Testing, Vol. 44, No. 5, pp. 367–374.

Pierce, Allan D (1989). Acoustics: An Introduction to Its Physical Principles and Applications. Acoustical Society of America, Woodbury, NY.

Ryan P. Carmichael (2009). “Relationships between Young’s Modulus, Compressive Strength, Poisson’s Ratio, And Time for Early Age Concrete.” Project Report, Swarthmore College, Department of Engineering.

Dr. Kimberly Kurtis. “Properties of Hardened Concrete”. <http://people.ce.gatech.edu/~kk92/hardconc.pdf> (July 30, 2015)

Thano Drimalas, Travis Lowe (2011). “Sulfate Attack: Do We Design for Chemical or Physical Attack?” Anna Maria Conference, University of Texas at Austin.

limewater - 3months

	Velocities (mm/µs)						avg vel	stdev	cv	Attenuation (dB/mm)						Average	stdev	CV
25	4.278565	4.444204	4.295987	4.299665	4.346757	4.388865	4.342341	0.064183	1.478078	0.3167641	0.230657	0.378552	0.311921	0.344256	0.330796	0.318824	0.049362	15.4824
50	4.358931	4.389055	4.323926	4.324484	4.29732	4.387152	4.346811	0.037498	0.862653	0.2598793	0.258134	0.326352	0.209511	0.316702	0.278212	0.274798	0.042867	15.59961
75	3.967941	4.254139	4.356931	4.323083	4.359728	4.098721	4.226757	0.160021	3.785907	0.3854765	0.33275	0.345398	0.366365	0.324187	0.382253	0.356071	0.025809	7.248245
100	3.960232	4.298913	4.381989	4.276667	4.290025	4.28142	4.248208	0.146329	3.444478	0.3977771	0.383157	0.28538	0.342946	0.353654	0.325727	0.348107	0.040469	11.62533
125	4.33559	4.185261	4.286013	4.309824	4.348324	4.373612	4.306437	0.066677	1.548317	0.3221083	0.378441	0.355577	0.34775	0.343448	0.312408	0.343289	0.023702	6.904296
150	4.02947	4.253521	4.30566	4.36576	4.420009	4.305462	4.27998	0.135448	3.164685	0.3247196	0.355473	0.24832	0.219909	0.239024	0.274227	0.276945	0.052853	19.08414
175	4.310475	4.330662	4.361052	4.351844	4.3159	4.297649	4.327931	0.024669	0.569989	0.2225259	0.307752	0.249051	0.301968	0.273625	0.326267	0.280198	0.03923	14.00078
							4.296924		2.122015							0.314033		

SS5 - 3 months

	Velocities (mm/µs)						avg vel	stdev	cv	Attenuation (dB/mm)						Average	stdev	CV
25	4.308372	4.381523	4.195012	4.285117	4.310241	4.239103	4.286561	0.064327	1.500663	0.340787	0.32214	0.341097	0.321951	0.26455	0.331437	0.320327	0.028602	8.929043
50	4.246479	4.307951	4.132608	4.329814	4.246715	4.334487	4.266342	0.076248	1.787187	0.3463077	0.239258	0.34624	0.219448	0.309443	0.304482	0.294196	0.053606	18.22113
75	4.238608	4.279148	4.296188	4.326858	4.251271	4.255518	4.274598	0.032928	0.770327	0.3430414	0.279297	0.282789	0.293773	0.302003	0.293238	0.299024	0.023066	7.713777
100	4.218557	4.177406	4.243791	4.296017	4.172829	4.1869	4.215917	0.047711	1.131679	0.313783	0.287025	0.334536	0.331837	0.344484	0.280988	0.315442	0.02636	8.356393
125	4.256762	4.249896	4.30256	4.238312	4.255499	4.217556	4.253431	0.028132	0.661403	0.3754033	0.372143	0.387204	0.358258	0.347913	0.34057	0.363582	0.017745	4.880665
150	4.317702	4.232933	4.283445	4.232327	4.192741	4.224094	4.247207	0.045185	1.063883	0.2690802	0.307888	0.259614	0.317445	0.277612	0.224372	0.276002	0.03382	12.25357
175	4.320643	4.035926	4.28727	4.205665	4.24557	4.082248	4.19622	0.114	2.716724	0.3309183	0.337474	0.253956	0.369937	0.273306	0.354079	0.319945	0.046091	14.40585
							4.248611		1.375981							0.312645		

Figure 14: Velocity and attenuation data of specimens for 3 months

limewater - 6 months																					
	Velocities	(mm/µs)						avg vel	stdev	cv	Attenuation	(dB/mm)						Average	stdev	CV
25	4.387111	4.417549	4.424162	4.400698	4.358138	4.349392		4.389508	0.030697	0.699327	0.330768	0.28945	0.23221	0.267804	0.3335	0.259455		0.285531	0.040497	14.18306
50	4.401758	4.415933	4.365418	4.461266	4.377894	4.420194		4.407077	0.034066	0.772975	0.275614	0.270109	0.301307	0.268903	0.284403	0.264339		0.277446	0.013563	4.888367
75	4.390543	4.37892	4.34777	4.352028	4.339965	4.337505		4.357788	0.021827	0.500866	0.324093	0.262582	0.320749	0.292427	0.295994	0.287562		0.297234	0.022774	7.66199
100	4.28145	4.320739	4.321552	4.294544	4.370435	4.35312		4.32364	0.033758	0.780788	0.345618	0.355759	0.325155	0.297767	0.314365	0.281676		0.320057	0.028129	8.788848
125	4.298246	3.959481	4.383472	4.403063	4.326733	4.292662		4.277276	0.161998	3.787404	0.39323	0.469945	0.254364	0.307127	0.343249	0.327967		0.349314	0.074523	21.3341
150	3.937647	4.338362	4.392372	4.245666	4.309473	4.313599		4.256186	0.163103	3.83214	0.401354	0.240437	0.224573	0.33164	0.290432	0.273496		0.293655	0.064905	22.10241
175	4.252226	4.382199	4.352174	4.407033	4.35052	4.375544		4.353283	0.053744	1.234568	0.318014	0.263839	0.204795	0.229404	0.278857	0.27449		0.261567	0.039787	15.21094
								4.337823		1.658295								0.297829		
SS5 - 6 months																				
	Velocities	(mm/µs)						avg vel	stdev	cv	Attenuation	(dB/mm)						Average	stdev	CV
25	4.161826	4.250318	4.31563	4.190097	4.253719	4.300387		4.245329	0.060154	1.416939	0.357926	0.314434	0.276138	0.405608	0.284744	0.319776		0.326438	0.048408	14.82902
50	4.24482	4.299871	4.178601	4.260536	4.240694	4.346187		4.261785	0.05697	1.33677	0.273932	0.284346	0.323802	0.315747	0.314214	0.294088		0.301022	0.019849	6.593779
75	4.195825	4.223109	4.332181	4.318103	4.254561	4.243232		4.261169	0.053606	1.258017	0.338342	0.380062	0.327052	0.362348	0.292182	0.343934		0.340653	0.030247	8.878978
100	4.256877	4.138683	4.301628	4.330164	4.207286	4.240084		4.245787	0.068333	1.609423	0.29824	0.36492	0.328685	0.323353	0.307554	0.379142		0.333649	0.031978	9.584199
125	4.139037	4.301411	4.228019	4.287179	4.33132	4.279693		4.26111	0.068666	1.611466	0.409461	0.346884	0.357214	0.328947	0.342629	0.356113		0.356875	0.027744	7.774235
150	4.294494	4.300942	4.337651	4.283397	4.285958	4.270259		4.29545	0.02316	0.539179	0.253429	0.303573	0.278718	0.27501	0.275841	0.242424		0.271499	0.021373	7.872043
175	4.268137	4.213836	4.260501	4.293464	4.247357	4.168116		4.241902	0.04462	1.051885	0.292247	0.339303	0.2619	0.258681	0.283723	0.309954		0.290968	0.030458	10.46769
								4.258933		1.260526								0.317301		

Figure 15: Velocity and attenuation data of specimens for 6 months

limewater - 12 months																					
	Velocities	(mm/µs)						avg vel	stdev	cv		Attenuation	(dB/mm)						Average	stdev	CV
25	4.559545	4.536022	4.491708	4.473826	4.507409	4.491487		4.509999	0.032014	0.709847		0.231283	0.194786	0.288394	0.305031	0.173341	0.219451		0.235381	0.051825	22.0173
50	4.478377	4.403956	4.514157	4.50991	4.447345	4.502695		4.476073	0.04321	0.965357		0.230961	0.278471	0.246914	0.254694	0.244752	0.239449		0.249207	0.016369	6.568483
75	4.408593	4.368627	4.424615	4.387746	4.426626	4.424349		4.406759	0.02384	0.540996		0.238663	0.222422	0.251341	0.24237	0.249132	0.242273		0.241033	0.010268	4.260009
100	4.419412	4.419127	4.421053	4.393076	4.411636	4.404741		4.411507	0.010928	0.247727		0.243466	0.241348	0.261905	0.250374	0.226078	0.252143		0.245886	0.012122	4.929815
125	4.441215	4.411067	4.41601	4.435071	4.44694	4.452889		4.433865	0.016893	0.380998		0.245885	0.251892	0.238732	0.248979	0.2525	0.240543		0.246422	0.005786	2.347999
150	4.490869	4.445035	4.453022	4.456483	4.474546	4.463839		4.463966	0.016552	0.370792		0.240032	0.26426	0.247647	0.243125	0.24634	0.250025		0.248571	0.008446	3.397815
175	4.436484	4.43634	4.416266	4.442724	4.511141	4.505415		4.458062	0.039948	0.896092		0.211037	0.23717	0.282178	0.215032	0.238072	0.215345		0.233139	0.026752	11.47478
								4.451462		0.587401									0.242806		
SS5 - 12 months																					
	Velocities	(mm/µs)						avg vel	stdev	cv		Attenuation	(dB/mm)						Average	stdev	CV
25			4.521876	4.443116	4.345321	4.28029		4.397651	0.106476	2.421191				0.200499	0.277972	0.224349	0.295026		0.249462	0.044411	17.80266
50			4.343723	4.426064	4.33937	4.293967		4.350781	0.055001	1.264171				0.219255	0.188361	0.288184	0.298954		0.248688	0.053517	21.51975
75			4.40518	4.44513	4.255076	4.264831		4.342554	0.096846	2.230151				0.255107	0.292485	0.314147	0.26925		0.282747	0.025993	9.192976
100			4.422281	4.510657	4.332186	4.258146		4.380818	0.10953	2.50023				0.203127	0.246111	0.30294	0.271318		0.255874	0.042156	16.4752
125			4.453457	4.551398	4.236853	4.352076		4.398446	0.13501	3.069487				0.277695	0.308073	0.347533	0.281256		0.303639	0.032251	10.62151
150			4.451885	4.46973	4.027644	4.370547		4.329952	0.20611	4.760091				0.229106	0.211567	0.352134	0.238545		0.257838	0.06385	24.76355
175			4.437086	4.443222	4.058491	3.218031		4.039207	0.576263	14.26674				0.271642	0.137692	0.377696	0.384463		0.292873	0.115637	39.48355
								4.319916		4.358866									0.27016		

Figure 16: Velocity and attenuation data of specimens for 12 months

limewater - 18 months

	Velocities (mm/μs)						avg vel	stdev	cv	Attenuation (dB/mm)						Average	stdev	CV
25	4.365811	4.316309	4.295377	4.345754	4.312931	4.319775	4.325993	0.025363	0.586292	0.264023	0.248583	0.310943	0.215354	0.291825	0.313533	0.274043	0.038549	14.06688
50	4.385153	4.294369	4.317262	4.31301	4.268739	4.227811	4.301057	0.052786	1.227278	0.258913	0.248361	0.259248	0.258835	0.26938	0.346896	0.273606	0.036515	13.34594
75	4.295979	4.242641	4.297216	4.284072	4.214526	4.252658	4.264515	0.033346	0.781945	0.233971	0.363763	0.278055	0.28134	0.3078	0.313063	0.296332	0.043373	14.63663
100	4.290901	4.266047	4.264343	4.206767	4.1875	4.251276	4.244472	0.039319	0.926352	0.254853	0.257375	0.264102	0.235329	0.326368	0.29903	0.272843	0.033458	12.26285
125	4.311426	4.286624	4.263493	4.292039	4.27903	4.251594	4.280701	0.021231	0.495972	0.298894	0.299158	0.269139	0.277723	0.27833	0.320872	0.290686	0.019159	6.590939
150	4.249045	4.282378	4.284737	4.326898	4.230543	4.270709	4.274052	0.033184	0.776399	0.227659	0.262766	0.257434	0.267698	0.282418	0.235953	0.255655	0.020431	7.991448
175	4.361776	4.317521	4.307692	4.274112	4.332329	4.261814	4.309207	0.037006	0.858777	0.206607	0.241512	0.249401	0.247427	0.234499	0.273699	0.242191	0.0219	9.042292
							4.285714		0.807574							0.272194		

SS5 - 18 months

	Velocities (mm/μs)						avg vel	stdev	cv	Attenuation (dB/mm)						Average	stdev	CV
25	4.129325	4.131796	4.101431	4.114122	4.077299	4.150435	4.117401	0.025747	0.625329	0.288251	0.269139	0.290187	0.269407	0.342247	0.269596	0.288138	0.028241	9.801045
50	4.020016	4.125244	4.184814	4.055511	4.108562	4.066478	4.093437	0.05856	1.430573	0.310695	0.253832	0.239258	0.29973	0.289161	0.259171	0.275308	0.028502	10.35275
75	4.038616	4.118609	4.156741	3.940598	4.163621	4.122281	4.090078	0.085669	2.094568	0.338645	0.285998	0.298478	0.337426	0.233393	0.30659	0.300088	0.038916	12.9683
100	4.065209	4.091758	3.832762	4.102007	4.126078	4.125461	4.057213	0.112287	2.7676	0.303876	0.270887	0.38366	0.282633	0.251816	0.24349	0.289394	0.050996	17.62182
125	3.745244	4.058374	4.147797	4.172083	4.132238	4.171429	4.071194	0.165062	4.054393	0.418285	0.357107	0.317618	0.294617	0.244484	0.285884	0.319666	0.060914	19.05559
150	4.100696	4.149567	4.211273	4.192776	4.178349	4.182121	4.16913	0.039128	0.93851	0.354362	0.289941	0.247868	0.249424	0.266031	0.238616	0.274374	0.04316	15.73019
175	4.097751	4.118464	4.176738	4.209283	4.239815	4.251057	4.182185	0.063274	1.512943	0.3683	0.305495	0.242791	0.264635	0.23576	0.235633	0.275436	0.052665	19.12067
							4.11152		1.917702							0.288915		

Figure 17: Velocity and attenuation data of specimens for 18 months

limewater - 24 months

	Velocities (mm/μs)						avg vel	stdev	cv	Attenuation (dB/mm)						Average	stdev	CV
25	4.447205	4.436034	4.381659	4.360278	4.3964	4.428067	4.408274	0.034149	0.774666	0.277334	0.327313	0.268088	0.292036	0.236645	0.234204	0.272603	0.03516	12.89777
50	4.345022	4.317829	4.325581	4.32043	4.474978	4.400438	4.364046	0.062466	1.431376	0.288931	0.371035	0.298686	0.312593	0.247629	0.249627	0.29475	0.045703	15.50558
75	4.322581	4.278038	4.317031	4.321152	4.378662	4.446358	4.34397	0.059561	1.37112	0.243781	0.279107	0.324953	0.285544	0.262632	0.234336	0.271726	0.032681	12.02706
100	4.346736	4.296058	4.285653	4.277872	4.337375	4.361003	4.31745	0.035175	0.814728	0.298389	0.336093	0.283103	0.351139	0.300549	0.243878	0.302192	0.038281	12.66771
125	4.348315	4.353606	4.288388	4.277872	4.385727	4.35893	4.335473	0.042671	0.984237	0.290201	0.388146	0.353105	0.318313	0.279525	0.267221	0.316085	0.046824	14.81382
150	4.33736	4.316357	4.40498	4.366841	4.392622	4.42707	4.374205	0.042046	0.961215	0.323254	0.348965	0.29753	0.323866	0.257948	0.227565	0.296522	0.045731	15.42248
175	4.357977	4.405024	4.361987	4.347337	4.504955	4.433888	4.401861	0.060254	1.368832	0.290675	0.328164	0.270351	0.266985	0.231977	0.199467	0.264603	0.044868	16.95669
							4.363611		1.100882							0.288354		

SS5 - 24 months

	Velocities (mm/μs)						avg vel	stdev	cv	Attenuation (dB/mm)						Average	stdev	CV
25	4.240506	4.282051	4.284921	4.31828			4.28144	0.03186	0.744146	0.368159	0.319361	0.286113	0.262948			0.309145	0.04565	14.76639
50	4.208368	4.208648	4.145101	4.2569			4.204754	0.045847	1.090366	0.30523	0.399002	0.406901	0.267332			0.344616	0.069189	20.07722
75	4.250739	4.085912	4.223812	4.206449			4.191728	0.072859	1.738163	0.391261	0.3428	0.303785	0.269786			0.326908	0.052254	15.98437
100	3.981035	4.219	4.133005	4.182612			4.128913	0.104696	2.535681	0.383089	0.357677	0.334724	0.313277			0.347191	0.030023	8.647435
125	4.140279	4.175957	4.284799	4.185447			4.19662	0.061919	1.475438	0.421042	0.37952	0.294968	0.355653			0.362796	0.052675	14.51925
150	4.140336	4.168675	4.216898	4.238819			4.191182	0.044805	1.069024	0.408325	0.35579	0.260167	0.288672			0.328239	0.066764	20.33995
175	4.110614	4.229895	4.300471	4.345754			4.246684	0.102477	2.413116	0.323506	0.363329	0.252168	0.250249			0.297313	0.055669	18.72416
							4.205903		1.580848							0.330887		

Figure 18: Velocity and attenuation data of specimens for 24 months

Table 7: Young's Modulus and Compressive Strength Calculations for Limewater (LW) specimens.

Poisson's Ratio	0.3	**Density**	2323 Kg/m^3
			145 lb/ft^3
Months	**Average Velocity (Km/s)**	**Youngs Modulus (MPa)**	**Compressive Strength (MPa)**
3	4.320849888	32217.57666	44.78176439
6	4.357285642	32763.21981	46.3114747
12	4.450097229	34173.81886	50.38514185
18	4.285714001	31695.73922	43.34282652
24	4.361897281	32832.60801	46.50784568

Table 8: Young's Modulus and Compressive Strength Calculations for 5% sodium sulfate (SS5) specimens

Poisson's Ratio	0.3	**Density**	2323 Kg/m^3
			145 lb/ft^3
Months	**Average Velocity (Km/s)**	**Youngs Modulus (MPa)**	**Compressive Strength (MPa)**
3	4.248610981	31149.31122	41.86126568
6	4.2589332	31300.8528	42.26956707
12	4.312435532	32092.21882	44.43395277
18	4.118318724	29268.09272	36.95764623
24	4.205902964	30526.21866	40.20327948

VITA

Meher Sri Lalitha Mandavilli

Candidate for the Degree of

Master of Science/Arts

Thesis: ATTENUATION IN CONCRETE

Major Field: Civil Engineering

Biographical:

Education:

Completed the requirements for the Master of Science/Arts in your major at Oklahoma State University, Stillwater, Oklahoma July, 2015.

Completed the requirements for the Bachelor of Science/Arts in your major at Osmania University, Hyderabad, Telangana/India in 2012.